Below please find our comments to the **Anonymous Referee #1**, which are shown in Italic.
Note: at the end of this document, are available two new sections and a new figure that will be added in the revised manuscript, according to our replies to the two referees.

Summary statement

1. *Unfortunately, the data is presented without sufficient context to allow the reader appropriate information to assess the processes proposed. This renders the main conclusions regarding multiple Alpine metamorphic events unjustified, or extremely difficult to support based on the uncertainties within the data set. The manuscript requires the presentation of the complete methods utilized, …*

We recognize that the two companion papers depend on each other, as well as two already published papers, for much of the data and methods used. In our revisions, we emphasize this interdependence and add specific pointers to the necessary information and its source. As for methods, we used in particular two programs (XMAPTOOLS 2.2.1 and GRTMOD). The approach was presented by Lanari et al. (2014, 2017); most of the details needed in the present manuscript are also discussed in these papers.
By adding a chapter at the outset, we expect that the doubts and difficulties this reviewer had in following our paper are now resolved. We also provide a summary on the methods used and the uncertainty estimation in the data set (chapter **5.2 Modeling phase equilibria in partially re-equilibrated rocks** in the revised version).

2. *… together with greater contextualization of the behaviour of other minerals within the rock to appropriately understand garnet and therefore eclogite evolution.*

The behaviour of the other minerals is presented extensively in the companion manuscript "Deeply subducted continental fragments: II. Insight from petrochronology in the central Sesia Zone (Western Italian Alps)", which is currently under review in Solid Earth and thus fully accessible. In the present manuscript, we specifically focus on garnet microtextures, thus adding this body of information again here would seem redundant.

3. *I understand that some of this information is presented in second installment or in different papers, if the data is reutilized it is not appropriate and leaves this manuscript with no novel quantitative information.*

The manuscript has an entire dataset that represent novel quantitative information not published elsewhere: the high-resolution compositional maps are based on well over two million EPMA analyses! The power of such maps to quantify the textural and microchemical archive in complex rocks is well established, so we are unsure what this reviewer is doubting here: The data we present are fully quantitative and entirely novel, i.e. they have not been presented elsewhere. We consider them the backbone to our modelling that lead us to unravel the fundamental processes – repeated growth and partial dissolution of garnet at high pressure conditions – and hence they are the core of the present paper.

Specific comments

4. *The main conclusions ascribing two periods of garnet growth/resorption during the high-pressure Alpine metamorphism is largely unconvincing.*

Further to the summary statement #3 we note that it is the combination of garnet textures and compositions presented, which indicate (at least) two discrete growth stages postdating the (pre-Alpine) core. Growth conditions (i.e. high pressures) were obtained by detailed thermodynamic modelling. Lobate textures and peninsular features inside the previous garnet generations revealed partial resorption, which in one sample also produced atoll garnet. The conspicuous microstructural evidence combined with the modelling results strongly indicate at least two high-pressure stages of garnet growth/resorption during Alpine time. We are unaware of any study ascribing comparable dissolution features to a process other than interaction with a reactive fluid.

5. *The P estimates established for rims2 and 3 are extremely similar, and within uncertainty estimates shown in Figure 8b. It is unknown how these estimates where determined outside of using a program GRTMOD making them hard to believe. What thermobarometry did the program use? What uncertainties are there on the method? What equilibrium volumes were assessed? This information together with the presentation and discussion of the complete thermodynamic models used, and their parameters is needed to justify the estimates provided. The presentation of pseudosections would also provide greater context to the history of the rocks.*

These questions showed us the need to give some details here. So, in our revised version, we introduced a chapter explaining the approach and details of the methods used, including the uncertainties in the data set. As stated in **5.2 Modeling phase equilibria in partially re-equilibrated rocks** in the revised version,

thermobarometry is based on isopleth intersection, and Lanari et al. (2017) explain how *GRTMOD* implements the estimates. Furthermore, our companion paper gives the details of garnet modeling (in supplement S8: GRTMOD results). Briefly, GRTMOD uses an inverse modeling approach; written in MATLAB©, it interacts with Theriak (de Capitani & Brown, 1987) using the Theriak_D (Duesterhoeft & de Capitani, 2013) extension. Specifically, for the samples presented here, the parameters chosen were given in **5.1.2 Garnet thermobarometry using GrtMod** section of the companion paper and also addressed in the revised version in the new chapter **5.2**. The equilibrium volume is assessed in a section of the companion paper (**5.2 Bulk rock and reactive bulk composition**), and P-T isochemical phase diagrams (pseudosections) are presented and discussed in that same paper (**5.3 Garnet thermobarometry and phase diagrams**).

6. *In particular, the questions surrounding what reactions are controlling garnet growth/resorption? What is the shape and habit of its isopleths? what part of the rock volume was equilibrated? These become difficult to assess in its current form, particularly by the assertion of fluid ingress. The influence on fluid needs to be discussed more fully in terms of the modelling volumes. If the equilibrium volumes are dependent on the diffusion of certain elements additional modelling of chemical potential gradients would be of potential benefit.*

(Please note that the first questions were partly addressed in the point above.) While textural and chemical evidence indicates that external fluid repeatedly interacted with nearly dry protoliths at HP conditions, we have no tight constraints on how much fluid entered at what spatial and temporal intervals. However, for each growth stage (within any one sample), the composition of garnet produced is uniform in each grain analysed, whereas the local geometry differs to some extent. This allows a spatial estimate of the reaction volume: Interaction of hydrous fluid with the reactive part of the assemblage (i.e. the matrix minerals) must have been at the scale of a thin section (centimetres) at least (except for the garnet relics left by incomplete reactions). Apart from garnet and local accessories (zircon, monazite), no mineral relics of the successive replacement reactions have been detected, indeed these rocks appear otherwise well equilibrated at eclogite facies conditions. Our modelling indicates that garnet resorption was dictated by changes in the PT conditions. As far as the suggestion to model diffusion based on the preserved chemical potential gradients in garnet, the complex and clearly diachronous overgrowth pattern would make this task extremely challenging, and we did not make such an attempt.

7. *In terms of the textural evolution of garnet, greater context of the surrounding phases is required to completely assess the rocks evolution, from both a microstructural and chemical perspective.*

We refer (as stated in the summary comments) to our companion paper, where the role of the other phases and their chemistry is extensively discussed.

8. *The sampling is from diverse compositions and protoliths, but consideration of the similarity of the processes is not adequately provided. It begs the explanation of how the period of brittle fracturing is linked to any remnant of current fabrics and their prevailing strain distribution locally and regionally? This manuscript largely states the processes of dissolution and precipitation without providing sufficient evidence to support and disprove possibilities. Presentation of quantitative microstructural information would greatly improve the submission and support some of the conclusions. Much of the focus is on garnet chemistry and not the rocks microstructure.*

These ambitions indeed have posed serious issues, all along the study presented here. Regrettably, the Sesia Zone presents limitations on them, and we may not have emphasized this sufficiently, though we address it repeatedly in the manuscript, e.g. on page 1, line 21: “Replacement of the Permian HT assemblages by hydrate-rich Alpine assemblages can reach nearly 100%” and on page 10, after line 23: “Apart from garnet and these accessory relics, the main pre-Alpine HT assemblage has completely re-equilibrated at eclogite facies conditions.”.

Pre-Alpine or other pre-eclogite facies fabrics are otherwise hardly preserved in the study area. Specifically, the brittle stages visible – at micron scale – in garnet cores could not be directly linked to locally or regionally prevalent strain patterns. In the revised version, we shall emphasize these points some more, to clarify explicitly the limitations imposed by the polymetamorphic and polydeformed setting of this study.

It’s not clear to us what "quantitative microstructural information” the reviewer would want to see. Our X-ray maps are based on quantitative data, and the information they contain is distinctly microstructural. Our study did not include PO fabric or grain size analysis etc., since we deem microchemical data to be far more relevant for the present purpose.

Technical corrections

Technical corrections: Page 1 Line 20: "...Sesia Zone, with a general decrease in fluid-garnet interaction observed towards the external areas"

Ok

Line 22: 100% of what?

Of the total, rephrased

Line 23: what deformation structures? need to look at other phase than just garnet, and even then, you have only talked about brittle fractures. What about crystal plasticity?

Here we meant deformation structures seen in the field, such as shear zones. We will rephrase this sentence to clarify what strain we address here.

Page 2 Line 2: may alter the zonation recorded by garnet

Ok

Line 3: diffusion is also dependent on the medium or deformation i.e. grain boundary fluid or pipe diffusion

Here we explicitly referred to intracrystalline diffusion in garnet.

Paragraph 2: the introduction needs a clearer statement about what the manuscript is trying to solve

Ok, we will strengthen this message (also in view of Ortolano's comments)

Line 18: Permian high-temperature and Alpine high-pressure events. How have these events been determined in age?

Here we refer to data in the published literature (references cited).

Line 19: minerals shouldn't be pluralized

Ok.

Line 20: clumsy sentenced would benefit from rewording

Agreed.

Line 32: this is an interpretation and needs to be stated as such

Ok, rephrased.

Line 33: jumps to generalities of garnet growth from specifics of Alpine rocks, needs to be clearer and explicit following one logic flow then the next

Good point, logic straightened.

Page 3 Second paragraph: at this stage, it is not clear how you propose to evaluate these possibilities, and exclude different scenarios that lead to your preferred interpretation

Ok, added a sentence in the revised version

Line 9 and 10: confusing sentence needs rewording. As it reads it seems you collected the samples away from the foliation?

Changed: We simply replaced “perpendicular to” by “across”, which should avoid confusion.

Line 11: delete single

Ok

Line 12: is the quantitative data already published? This is a major flaw and is not appropriate.

In this sentence we referred just to the quantitative pressure and temperature data that are part of the companion paper. These data are used in this manuscript in relation with the microstructures, as we wrote. All the quantitative high-resolution compositional maps presented in this study are entirely novel. Please, see reply to summary statement 3

Line 23: delete but

Ok

Page 4 Line 3: overprints

Ok

Line 4: granulite facies conditions and retrograde amphibolite facies conditions

Ok

Line 13: latter? Be explicit

Ok, changed to “maps”

Line 15 replace were with involved

Ok

Line 22: present the end member formulae used throughout

Ok

Line 24: ...representative amounts of the samples

Ok

Line 30: quantify size range

It is from sub-millimetric to a few centimetres, we will add this information in the revised version

Page 5 I think the use of rim doesn’t really apply, they are interpreted growth zones. Using rim makes distinguishing the processes and stages difficult, as in most instance they are not physically rims. The microstructures, need more detailed descriptions and not left in the supplement. Grains sizes should be quantified. Requires photomicrographs

Rim seemed the best term found to describe such growth zones, as most of them surround garnet cores. (Perhaps “seam” would be an alternative, but not clearly better suited.) Note that we specify “internal and external rims”, where appropriate. (See pg.6, line 16 below.) We could indeed add a description regarding microtextures here, rather than in the supplement. No problem either to add a plate with photomicrographs showing the microstructures, if an additional figure is deemed necessary.

Line 2: are these exsolution needles? If so this could be of significance to temperature or pressure estimates

No, we think that these are fine inclusion of rutile that is abundant in our samples (1-2%) and in equilibrium with the eclogite facies fabrics. The origin or precise growth process remain uncertain.

Line 6: from the internal and external areas

Ok

Line 23: sentence needs rewording

Rephrased

Line 30: I am not sure this is completely true, EBSD provides quantitative information about garnet microstructures, X-ray maps provide links between chemistry and textures. Deleting the word most would help this sentence.

Ok, modified according to the comment

Page 6 Line 1: change pictures to images

Ok

Line 10: How was the sealed fractures accounted for in the fractionated compositions and the modelling procedures?

The sealed fractures have been not considered in modelling because of their small size and low abundance in terms of volume%. However, we observed that their composition matches that of Alpine rims (specifically of Rim2 in sample FG1315). Owing to the low modal abundance these fillings were not fractionated from the bulk rock to model the next growth zones. We can specify this in the revised version.

Line 16: how is this accounted for? Growing in two directions

In the revised version we will add some information and clarify the wording, as "Rim2 ($Alm_{64}Prp_{24}Grs_{11}Sps_{1}$) is found as three textural types: (a) It grew externally onto Rim1; (b) between core and Rim1, and also surrounds the Rim1 peninsula, thus extending it (by ~20 µm); (c) fine veins (5-20 µm thick) dissecting Rim1 also show Rim2 composition (as discussed in section 6.2). The outermost rim (Rim3) is lower in grossular ($Alm_{69}Prp_{24}Grs_{6}Sps_{1}$); it displays peninsular growths inside Rim1 and Rim2. Remarkably, Rim3 is thin (~100 µm) parallel to the main foliation and thicker (~400 µm) perpendicular to it."

Line 19: providing some quantification of the growth scale in particular directions would strengthen conclusions, particularly across the diverse samples. However this does not explicitly consider crystallography

See reply above

Line 24: Almandine and spessartine vary a lot in the cores?

Yes, this is shown in Fig. 5; and in the zoning profile of the garnet end-member in Fig. 2 of Lanari et al., 2017.

Page 7 Line 2: the sealing of the fracture pattern is not obvious on the element maps?

Yes it is: the compositional maps have a resolution high enough to display this change in chemistry between the garnet core and the garnet sealing the fracture pattern. Furthermore, and such difference is chemistry is constant in different areas of the garnet. A technical detail, the maps have step sizes between 3 and 5 micrometres and most of the fractures have a width that is at least three times major.

Line 10: again, not obvious what this is talking about; the pyrope contents are unevenly distributed why is this so?

This important observation is but described here; the interpretation and discussion are presented in **6.3 Re-equilibration close to fluid pathways**

Line 17: remove interpretative statements in the results section

Ok

Paragraph 3 No results for the thermodynamic modelling are presented, this is more so thermobarometry. The models should be shown and the methods used to estimate P-T discussed. What parts of the garnet were fractionated (supplement figure maybe), how did this vary throughout the rest of the rock volume, garnet does not grow in isolation. No equilibration context is provided, it would be good to know the reactions controlling the growth/resorption. What are the nature of the garnet isopleths? Was fluid added and how did it change the modelling? These questions are not explicitly addressed. Discussion of the uncertainties of the P-T estimates are fundamental to resolving these discrete events, currently they are within errors presented in Figure 8 and cannot be resolved. The way this reads it seems the data has been presented elsewhere and therefore is largely re-interpreted and not appropriate as central conclusion of this manuscript, what is new here?
Critique accepted. Please refer to the **Summary statement** and **Specific comments.** There we clarify that in this paper we link our microchemical and -textural data (presented in this manuscript) to our PT-data (presented in the companion manuscript). Whereas we are in doubt about the need to repeat details of the approach and models presented there, we do refer to the new paragraph introduced above.

Page 8 Line 2: don't start a sentence with and

Deleted "and"

Line 7-14: there is an extremely large variation in pressure across all samples, encompassing the entire range of the high-pressure event, how can these be resolved as discrete metamorphic episodes?

This is the range of all the P data, the single values are presented in Fig. 8. Each growth zone of garnet has a distinct chemical composition that suggests a series of metamorphic episodes related to changes in P,T and reactive bulk rock. In the area we studied, this is also reflected by several metamorphic and deformation stages occurring at eclogite facies conditions, such as the presence of a relic eclogite facies foliation preserved in microlithons and wrapped by the main eclogite facies foliation.

Line 17: there is no U-Pb ages presented?

No, but ages from the same samples set are presented in Kunz et al. (2017). Rephrased for the sake of clarity.

Line 30: replace fillings with more indicative terminology

Replaced with crack fillings

Page 9 Line 1: veins? Keep terminology consistent

OK, changed

Line 4: best observed, delete visible. But less so for Mn

Done

Line 5: if concentration limits are near the lower limits of detection this should be discussed in the results

Ok, added a sentence about it.

Line 6: yes, grossular is commonly pressure dependent, but this should be show specifically for these samples together with the nature of garnet modes to assess potential resorption.

See our reply to summary statement 1 and specific comment 5. In detail, this material is available in our companion paper (in supplement S8: GRTMOD results).

Line 8: sentence needs restructure as it is confusing in its current form

Rephrased

Line 9: these options should be presented as possibilities unless direct evidence is shown to support different possibilities. Sentence also jumps from small-scale to large earthquake features

This **is** presented as a possibility here ("may have been related…"); the jumps from small-scale to large earthquake features is what the reported studies advocated. We merely cite these studies as a possibility to explain the observed small-scale features.

Line 10: referencing an in-preparation manuscript is bad practice and not appropriate and should be removed. Is there evidence to support difference in rheology to the matrix phases?

At this stage this manuscript is still under review in G^3. We expect an editorial decision shortly and will update this reference or delete it if need be.

Line 15: how do you know that fluid was introduced? Needs some direct evidence

We consider the fracture networks in high-temperature garnet (cores) filled by high-pressure garnet as direct evidence. Less direct, but equally essential, is the volatile content of the rocks: Their pre-Alpine protoliths were granulites, i.e. essentially anhydrous rocks, whereas now they are micaschists containing up to 2 wt% H_2O (see Table S1). If pre-Alpine rehydration had happened, e.g. say tectonic extension-related fluid had substantially hydrated the HT-protoliths, one would expect to see evidence of such as garnet alteration. Yet this is completely absent in all but one of our samples (see Fig. 9), in which a thin pre-Alpine (low-Ca) rim grew. Pre-Alpine hydration thus happened but locally and to a very limited extent. These lines of evidence jointly demand the introduction of substantial volumes of hydrous fluid, clearly in several episodes (on account of the different garnet rims), in the subducted slab.

Lines 18-26: some of the fractures are accompanied by distinct Xalm and Xsps contents comparatively to the high-pressure rims, how is this accounted for under a high pressure and not a low-pressure event. Presentation of modelling would aid this discussion

We disagree: The X_{Alm} and X_{Sps} in the sealed fractures are in the range of the high-pressure rim compositions we calculated by thermodynamic modelling. This is shown at page 6 lines 13, 27; page 7 lines 4, 14.

Line 29: add the, before the word most

Ok

Page 10 Line 1: what other possibilities could there be that could be discounted?

We did address these questions: On page 9 line 33 we stated "we surmise that Rim1 and 2 are not a simple growth sequence, with the older generation in a more internal position and younger ones more externally." We also discuss (and dismiss) the possibility that these growth features are related to a pressure cycling because we observe veins that resorbed Rim1 and connected the internal and external parts of Rim2. Perhaps these considerations are worth repeating in this part of the discussion (also in view of the comment below (line 8).

Line 3: some of these zones are barely present

A careful look at the figures shows that in samples FG12157 and FG1249 all zones are well visible.

Line 8: present the evidence to support this and discount the other possibilities, otherwise it feels a bit like special pleading

Ok, we can add this to the discussion in the revised version.

Line 31: this possibility should be discussed in light of other potential ways to resorb garnet, i.e. P-T paths involving consumption. This becomes impossible to evaluate as the modelling is not shown and it is unknown if water was added or subtracted from the modelling

Not clear what "this possibility" refers to. However, as modeling is a central topic in the companion paper, which discusses garnet resorption in response to changes in P-T, readers interested in evaluating the models will want to refer to that paper. We propose to point to the models, at this point in the revised manuscript.

Page 11 Line 10: best observed

Ok, changed

Line 14: if this is re-equilibrating, what phases is it adjusting with? i.e. what is the volume and how can the P-T be robust if the equilibrium volume is a few microns within a garnet grain with introduced fluid

Here we address intracrystalline re-equilibration inside the garnet core and specifically around the fractures. This situation differs from the equilibrium volume with a surrounding matrix. The reviewer's concern about PT-estimation is legitimate, but is it essential to explain the details here? The strategy used is fully explained in Lanari et al., 2017, as well as in the companion paper. We could state here that PT-estimates were based on the composition of unaffected areas of the core and the newly grown areas of the rims. However, some readers would probably find such detail to be out of context.

Page 12

Line 7: the mineral equilibria modelling has not been shown and the paragenesis have not been outlined, these need to be discussed instead of sorely garnet chemistry

These details and data are fully discussed in the companion paper. We will rephrase this sentence and add a reference of the companion paper

Line 10: jumps to the gross scale. A clear picture of the relationships of the different samples and their degree of change should be provided to aid the reader

This is extensively set out in the previous sections, but we probably should add a sentence here to summarize the spatial relation of the samples.

Page 13 Line 24: this study does not show or discuss zircon, so how can we know it has brittle deformation features in its cores?

This is correct. We propose to refer to a companion paper dealing with zircon, thus modifying the text (lines 23-25): In the sample suite reported here, pre-Alpine conditions are evident in garnet cores and relic zircon (Kunz et al. 2017). The relic features show brittle deformation textures, i.e. cracks, but no displacement.

Line 33: if the diffusion of the different element influenced the re-equilibration volumes, then discussion and presentation of chemical potential gradients would aid the understanding of the potential re-equilibration processes

Diffusion always influences the re-equilibration volume. A specific discussion in the present situation is outside the scope of the present paper and would be challenging given the complex zoning textures in the samples presented. Specifically, estimating the re-equilibration volume in the core is challenging, given the

high density of fractures, their complex 3D geometry, the repeated interaction with fluid at changing PT-conditions, etc.

Figures

Figure 1. If all samples are from the internal complex how can it be known what the difference in ingress occurred in the external complex?

This manuscript does not presented data for the External Complex, so implications on this unit are outside the scope of the present paper. We refer the reader to our companion paper for the geological evolution of the External Complex and its relations to the Internal Complex. The reason to omit the External Complex here is that it is composed mostly of orthogneiss that rarely contain garnet in the main paragenesis.

Figure 2: should be all photomicrographs to discuss the texture then presentation of chemical maps. Additional photomicrographs of the general textures observed throughout the samples would provide better context to the garnet microstructure and evolution of the samples.

Ok, good suggestion, we will add such photomicrographs (see at the bottom of this document)

Figure 3: in many of the captions, interpretations are presented as facts. Interpretations should be avoided wherever possible in figure captions

Ok, we will modify them according to this comment and indicate interpretations as such, where they are included.

Figure 6: avoid interpretations in the caption, especially surrounding re-equilibration it is not known what proportion of the rock volume is in equilibrium

Ok, as above.

Figure 8: where is the data from? How was it collected? if the data is from a previous publication this is inappropriate. What method was used to determine the P-T? what are the uncertainties? The high-pressure event overlaps suggesting any discrete events are not resolvable

As stated in the caption, we summarize relevant data from Lanari et al., 2017 and Giuntoli, 2016, so as to use them to distinguish Alpine from pre-Alpine growth zones. As stated above, we will introduce a brief section on modeling in this paper.

Figure 9: This figure is inconsistent with Figure 8. How is rim1 formed at low-pressure but it is present as a high-pressure stage? Rim2 and rim3 are within error and likely reflect one in the same process. The garnet modes have no context without the pseudosection, how is it know the water was introduced specifically at this time, was this incorporated into the model parameters?

The two figures actually are consistent: Sample FG1249 is the only one in which a pre-Alpine rim (pink square in Fig.8 a, b) was detected. We discuss this in the text and propose that Rim2 and Rim3 represent growths triggered by fluid influx, likely reflecting one and the same process. Select details about modeling will be introduced in the manuscript, as stated above, but for all of the information requested in this comment, the companion paper is indispensable.

We thank the Anonymous Referee #1 for so many constructive comments.

Francesco Giuntoli, Pierre Lanari, Martin Engi

Below are available two new sections and a new figure that will be added in the revised manuscript, according to our replies to the two referees.

New title of paragraph 4: "**4 Sample selection strategy and petrography**"

(Paragraph to be added after line 5 page 5)

These petrographic features match observations reported by previous authors (see references in section 1) who had attempted to distinguish Alpine form pre-Alpine garnet in the Sesia Zone. In light of these observations, the sample selection strategy we adopted for this study used the following criteria:

- The presence in hand-specimens of garnet of diverse sizes (sub-millimetric to a few centimetres);
- The bimodal distribution of garnet in one and the same thin section, with the larger crystals displaying a bright core and dark rims, as illustrated above, and smaller euhedral crystals (Fig. 2);
- Bright cores surrounded by darker rims evident in the SEM with a BSE detector.

This list of criteria was adopted to investigate the widest possible range of microtextures and processes recorded by garnet. Applying the list lead us to concentrate on only ~5% of the total samples taken, mostly because larger (pre-Alpine) garnet grains rarely survived in the area of study. In fact, almost all of the pre-Alpine HT assemblages had re-equilibrated in hydrate-rich Alpine assemblages.

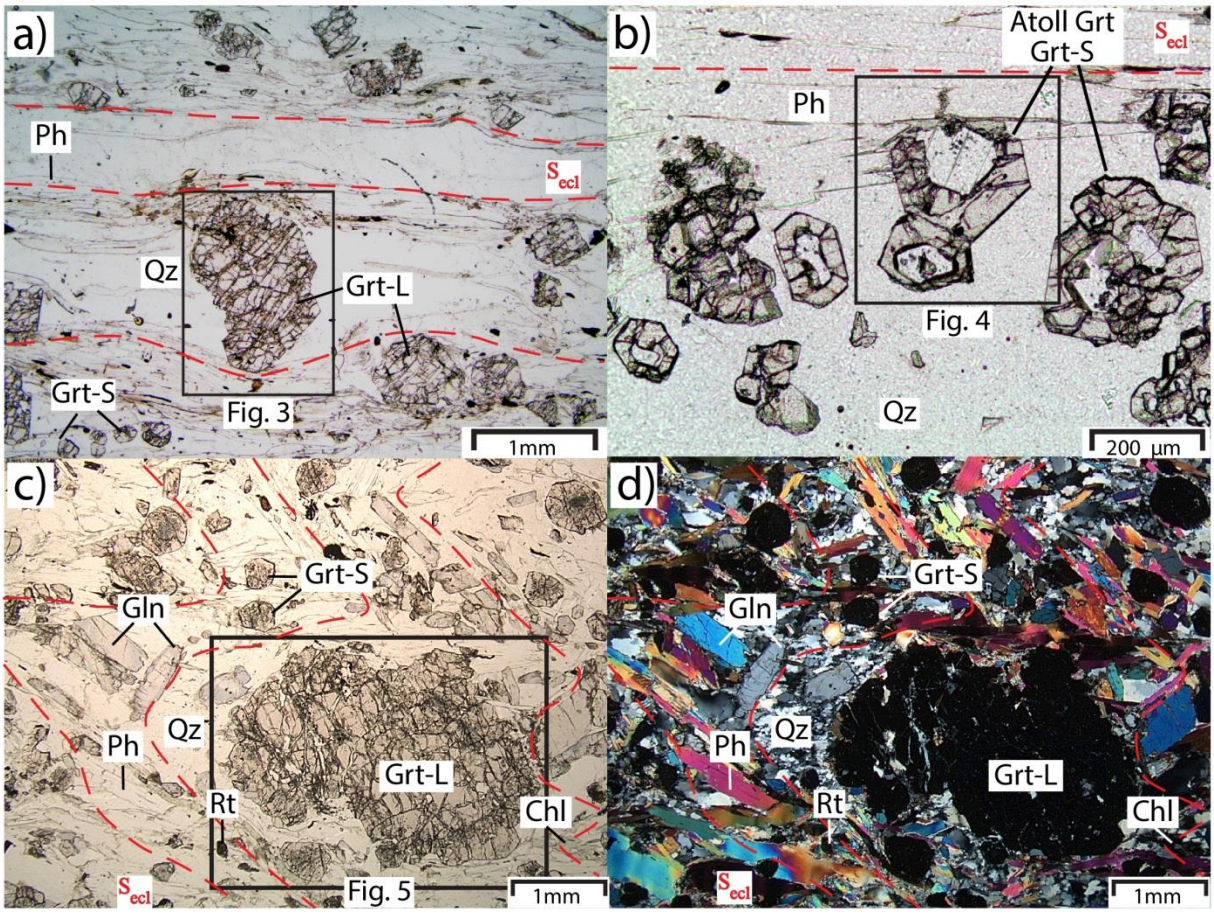

Figure 2: Thin section optical microphotos displaying the eclogitic foliation (S_{ecl}, red dashed line) and the bimodal size range of garnet (large garnet grains Grt-L; small garnet grains Grt-S; see text for further details). Black squares indicate the location of the high-resolution X-ray maps. (a) S_{ecl} wrapping Grt-L grains in sample FG1315. (b) Same thin section as (a) with atoll garnets (Grt-S) located within a Qz rich band and a Ph rich band. (c) and (d) Folded S_{ecl} marked by Ph, Gln and Rt; Chl is present in the fold hinges. Plane-polarized light: (a, b, c); cross-polarized light (d).

5.2 Modeling phase equilibria in partially re-equilibrated rocks

In each sample investigated, several garnet growth zones were identified by careful analysis of the end-member proportion maps using XMAPTOOLS (Lanari et al., 2014). For modelling, representative areas of each growth zone were extracted from this dataset, using the program's export function to obtain average chemical compositions. The quantitative micro-mapping strategy employed in this study has well established advantages (e.g. Marmo et al., 2002;Lanari et al., 2013;Ortolano et al., 2014;Angiboust et al., 2016) over traditional spot analyses: (1) it allows key relationships, such as the successive growth zones, to be identified and relevant compositions to be constrained, (2) it permits testing if chemical zoning patterns are consistent over several grains, which helps support (or refute) the assumption of grain boundary equilibrium, (3) it can be used to approximate local reactive bulk composition by accounting for mineral relics. In all the samples of the present study, the growth zone patterns and compositions of the mineralogical phases were consistent at thin section scale.

The complexity of the garnet compositional zoning shown in Figures 3, 4, 5, 6 indicates that isochemical phase diagrams (or pseudosections) must be used with due caution. Previous studies have demonstrated that garnet fractionation can sensibly affect the reactive bulk composition (Evans, 2004;Robyr et al., 2014;Konrad-Schmolke et al., 2008) and thus shift the calculated garnet isopleths in a P-T diagram (Lanari and Engi, 2017). However, garnet fractionation is not easy to account for where several growth stages are evident, as well as intermittent dissolution (which we show to be the case in the companion paper by Giuntoli et al., submitted). Since the older growth zones are but partially preserved, as indicated e.g. by lobate edges (Figs. 2, 3, 5, 6) in our samples, a novel strategy was developed (Lanari et al., 2017). It relies on the optimization of the reactive bulk composition, and the computer code (GRTMOD) presented in that study was applied to the present samples. In essence, for each garnet growth zone, the reactive bulk composition was optimized jointly with the P-T conditions to predict (using Theriak-Domino, de Capitani and Petrakakis, 2010) a garnet composition that matched the measured one. Results were accepted if the residual value (the sum of the fraction of end-members) between the modelled and observed garnet compositions was <0.05, reflecting a close match. Previously formed garnet generations were removed from the bulk rock composition, according to the end-member proportion maps analysis. Analogously, in the case of garnet resorption, the appropriate components were again added to the reactive bulk composition. This iterative modeling was applied to each successive growth zone. The resulting P-T estimates are reported in Figure 8b, with error bars showing the P-T uncertainty related to the analytical error of the garnet composition (Lanari et al., 2017). For any given reactive bulk composition, narrowly spaced isopleths return small uncertainty envelopes, whereas widely spread isopleths return larger ones. A detailed account of these methods and the internally consistent thermodynamic dataset used, including solid solution models, is presented in the companion paper (Giuntoli et al., submitted).

Here follows **5.3 Results of thermodynamic modelling of garnet growth zones** (page 7 line 20 of the submitted manuscript), previously number 5.2

References

Angiboust, S., Yamato, P., Hertgen, S., Hyppolito, T., Bebout, G., and Morales, L.: Fluid pathways and high pressure metasomatism in a subducted continental slice (Mt. Emilius klippe, W. Alps), J. Metamorph. Geol., 2016.

de Capitani, C., and Petrakakis, K.: The computation of equilibrium assemblage diagrams with Theriak/Domino software, Am. Mineral., 95, 1006-1016, 10.2138/am.2010.3354, 2010.

Evans, T. P.: A method for calculating effective bulk composition modification due to crystal fractionation in garnet-bearing schist; implications for isopleth thermobarometry J. Metamorph. Geol., 22, 547-557, 2004.

Giuntoli, F., Lanari, P., Burn, M., Kunz, B. E., and Engi, M.: Deeply subducted continental fragments: II. Insight from petrochronology in the central Sesia Zone (Western Italian Alps), Solid Earth, submitted.

Konrad-Schmolke, M., O'Brien, P. J., De Capitani, C., and Carswell, D. A.: Garnet growth at high- and ultra-high pressure conditions and the effect of element fractionation on mineral modes and composition, Lithos, 103, 309-332, 2008.

Lanari, P., Riel, N., Guillot, S., Vidal, O., Schwartz, S., Pêcher, A., and Hattori, K. H.: Deciphering high-pressure metamorphism in collisional context using microprobe mapping methods: Application to the Stak eclogitic massif (northwest Himalaya), Geology, 41, 111-114, 2013.

Lanari, P., Vidal, O., Lewin, E., Dubacq, B., De Andrade, V., and Schwartz, S.: XMapTools a Matlab©-based graphic user interface for microprobe quantified image processing, Computers and Geosciences, 62, 227-240, 10.1016/j.cageo.2013.08.010, 2014.

Lanari, P., and Engi, M.: Local Bulk Composition Effects on Metamorphic Mineral Assemblages, Reviews in Mineralogy & Geochemistry, 83, 55–102, http://dx.doi.org/10.2138/rmg.2017.83.1, 2017.

Lanari, P., Giuntoli, F., Loury, C., Burn, M., and Engi, M.: An inverse modeling approach to obtain P-T conditions of metamorphic stages involving garnet growth and resorption, Eur. J. Mineral., 29, 181-199, 10.1127/ejm/2017/0029-2597, 2017.

Marmo, B., Clarke, G., and Powell, R.: Fractionation of bulk rock composition due to porphyroblast growth: effects on eclogite facies mineral equilibria, Pam Peninsula, New Caledonia, J. Metamorph. Geol., 20, 151-165, 2002.

Ortolano, G., Zappalà, L., and Mazzoleni, P.: X-Ray Map Analyser: A new ArcGIS® based tool for the quantitative statistical data handling of X-ray maps (Geo-and material-science applications), Comput. Geosci., 72, 49-64, 2014.

Robyr, M., Darbellay, B., and Baumgartner, L. P.: Matrix-dependent garnet growth in polymetamorphic rocks of the Sesia zone, Italian Alps, J. Metamorph. Geol., 32, 3-24, 2014.

Here we reply to the comments of **Ortolano-Referee #2**. We reported in Italic the Ortolano-Referee #2 text. Note: at the end of the document "Reply to Anonymous Referee1" are available two new sections and a new figure that will be added in the revised manuscript, according to our replies to the two referees.

Summary statement

- *Although the work presents high-quality analytical data, unfortunately, the manuscript does not have a clear focusing line. It seems often a description of samples without sufficient context to allow the reader appropriate information to assess the processes proposed. The problem starts from the sample selection strategy. This is indeed not sufficiently justified to underline the specific peculiar features useful to better highlights the different mechanisms of garnet overgrowing stages developed during the Alpine evolution.*

Thanks for these suggestions: We will strengthen the Introduction, stating more clearly the specific goals of this paper. In the revised version, we will also change the name of Section 4 in "**4 Sample selection strategy and petrography**", we shall include a paragraph on important aspects of our sample evaluation strategy.

- *It is out of sense for instance, during discussion, uses the name of the sample to describe the specific textural characteristics of the related Alpine garnet overgrowing stages. For an external reader, a name is a name. Instead, should be better associate a name to a specific process.*

We understand that the sample names we use have no meaning to an external reader, but we think that keeping them in the text is important and fundamental to be able to discuss the different processes in the light of the garnet textures. Such textures have some similarities amongst samples but also remarkable peculiarities and differences. Without referring to the sample names, specific observation and discussion would result hard or impossible to follow to an external reader. It would also diminish the possibility of the reader to self-asset the interpretation of such textures and it would render the discussion section much more subjective to the eyes of an external reader. Furthermore, to give more result to the processes and less to the samples names, we already grouped the different processes as is visible from the different subsection of section 6 (**6.1 Micrometre-size fracture network in garnet cores, 6.2 Resorption and growth: fluid-related textures, 6.3 Re-equilibration close to fluid pathways**) and discussed similarities amongst samples for each of these. Finally, this sample series is part of other publications; some of these are already published and have this sample nomenclature: changing it would results to confusion and would damp comparison of the data.

- *Moreover, during in the introduction as well as in the discussion, were not taken into account any alternative possible interpretation for justifying the observed garnet texture. For instance, some brittle behavior can be generated not only by a high strain rate in non-coaxial regime but also by plastic-to brittle transition with the formation of a fractured mesh that might represent evidence of past episodic tremors or "slow earthquakes" triggered by high pore fluid pressure (Malatesta et al., 2017 Geological Magazine). What other evidence have the authors to justify their interpretation?*

This comment seems partially unfounded: In the Introduction, we outline three possible interpretations of the garnet textures reported in the literature from the Sesia Zone (page 2 lines 19-32); alternative processes leading to the formation of atoll garnet are presented (page 2 line 32, page 3 line 4). Furthermore, we propose two alternatives processes to account for the development of fractures (page9 lines 15-24). For reasons outlined in section 6.1 we favour the first interpretation. It is correct, however, that we can improve the discussion section by stressing which data and textures support or confute alternative interpretations (as referee#1 also commented).

Regarding the specific suggestion *(following Malatesta et al., 2017)* of *tremors or "slow earthquakes" triggered by high pore fluid pressure* possibly leading to brittle behaviour, we think that this situation applies to our dataset: The interpretation by *Malatesta et al.* is based on lithotypes with strong rheological contrast, i.e. metasediments alternating with metabasites, separated by cm-thick talcschist layers, so metabasite shows brittle fracturing (boudinage, brecciation) inside the weak matrix (Fig.4, 14). In our samples, brittle fractures are observed in garnet (and zircon) cores, which are relics of a dry granulite that must have been mechanically strong. We see strong analogies in our situation with the fracture patterns and compositional maps of garnet reported by Austrheim et al., 1996; Angiboust et al., 2012 and Austrheim et al., 2017. These authors interpreted such textures as produced by high strain rates related to seismic failure. For this reason we tentatively adopt such an interpretation to explain the features we observed in garnet (page 9 lines 9-11).

- *Finally, in my opinion, the potentiality of the quantitative data extrapolation from image analysis by X-Map tools, was not satisfactory, in term for instance of the extrapolation of the effective reactant volumes of the single observed paragenetic equilibria. This can be useful to better constrain the ab initio*

parameters useful for a more consistent thermodynamic modeling, which unfortunately, was not described in the manuscript.

As in our reply to Anonymous Referee #1 comments, these data are part of the companion paper "Deeply subducted continental fragments: II. Insight from petrochronology in the central Sesia Zone (Western Italian Alps)" currently under review in Solid Earth and fully accessible. We agree that these data are necessary to support our interpretations, but the volume and diversity of material is such that we decided to present it in companion papers. In the present manuscript, wherever data are particularly critical for our interpretation, we refer the companion paper (as Giuntoli et al., submitted). However, since both Ortolano and Referee#1 had difficulties to see the connection and asked for some clarification on methods we used, a section (**5.2 Modeling phase equilibria in partially re-equilibrated rocks**) will be introduced in our revised version to explain our approach to thermodynamic modeling of garnet.

- *For all of the above reasons, the manuscript requires a deep major revision, consisting in a substantially rewriting of the introduction and of the discussion part, focusing the attention for instance to the use of the image analysis in the calculation of the effective bulk rock chemistries for the single extrapolation of paragenetic equilibria. Moreover, it is fundamental a better presentation of the complete methods utilized, together with a greater contextualization of sample selection.*

We propose to improve the Introduction according to Ortolano's comments. For the use of image analysis in approximate effective bulk rock compositions from local composition, but we do not believe that this is necessary in this paper. The bulk rock composition was used for modelling, this is quite common and the good results of the models partially justify this assumption. The reproducibility of the zoning pattern at the centimetre scale also supports this assumption. It is thus not necessary to define a smaller equilibration volume that is also not supported from a textural point of view. The garnet composition is for instance the same in the phyllosilicate-rich layers and in the quartz-rich layers supporting the grain boundary equilibrium model assumed here. All these points are already discussed in some details in Lanari et al. (2017), presenting the GRTMOD program. A new modelling section with some computational details will be introduced in the revised manuscript (see previous comment). As stated above, we shall also add a section regarding the sample selection (collection and evaluation) strategy we used.

Specific comments (from Ortolano's pdf supplement file)

- *It is a zoning or an overgrowing crystallization*

To avoid misinterpretation at this stage, we prefer the "zoning" as a purely descriptive term.

- *Local texture and mineral chemistry are combined to define the ab inition constraints for a more consistent thermodynamic modelling. This last is function of the textural and mineral chemical features of the specific paragenetic equilibria*

Rephrased according to this comment.

- *Please introduce the sample selection logic, before to describe the chracteristic of the single sample. The sentence is not so clear, please rewrite.*

This is good advice and, as stated in the summary statement, we will adopt it.

- *This is the unique solution?*

See the above discussion in summary statement

- *Please emphasize that the thermodynamic modelling was assisted by quantitative image analysis useful to extrapolate the effective bulk rock chemistries of each paragenetic equilibria*

Ok, we introduce some details about modeling in the main text, as stated above

- *A robust thermodynamic modelling derives from a quantitative extrapolation of the effective reactant volumes of the single metamorphic evolutionary stage*

We present this topic in the new section about modeling

- *How many samples with what logical selection*

As above, we introduce this in the section on sample selection strategy

- *This is an anticipation of the discussion. Please avoid it.*

Ok, deleted.

- *How many thin sections. What is the logic of sample collection and more in particular, what is the logic of sample selection of those sample used for the thermodynamic modelling?*

We add this in the section on sample selection strategy

- *Please specifies better the logical meaning of the proposed procedure and the specific results that the authors want to reach for the aims of the present work.*

Ok, we will add such details, as well in the new section **5.2 Modeling phase equilibria in partially re-equilibrated rocks** that will be added in the revised version.

- *Also in this case, please specifies the logical meaning at the base of the use of XMapTools, such for instance to unravel the effective bulk rock chemistries of the modelled systems and so on.*

This will be presented in the new section **5.2 Modeling phase equilibria in partially re-equilibrated rocks** that will be added in the revised version.

- *Please specifies the logical process of the sample collection campaign and the following logical meaning of selection of those samples considered characteristic of....(e.g. Alpine prograde metamorphism; Retrograde Variscan metamorphism and so on...)*

Yes, we introduce this in the section on sample selection strategy.

- *More than a compositional zoning, I would talk about Evolution of the garnet overgrowing stages*

We consider this suggestion as a good alternative

- *This fractures are very intersting. Just for suggestion, if you use the X-ray Map Analyser (Ortolano et al., 2014 C&G), you can probably extrapolate the specific principal component of the classified image which correspond to the different generation of sealed fractures.*

That's correct, and in fact we followed this suggestion but using XMapTools; the results are presented in section 5 (e.g. page 6 line 13). A clarification: we see one generation of fractures sealed by garnet, a second generation is cutting across all of the garnet growth zones with chlorite lining. This is related to the retrograde greenschist stage, a late metamorphic phase evident in many parts of the Sesia Zone.

- *Principal Component Analysis indeed can highlight the specific interdependence of the different elemental components, emphasizing the presence of specific subphase, using the second analytical cycle of X-Ray Map Analyser.*

Ok this is true, but it can also be achieved in a simple binary chemical diagram, as only two chemical variables are independent in this case (XAlm and XGrs for instance with XPrp being dependent).

- *It is out of sense indicate a subparagraph of the manuscript with a samèle name. An external reader would understand the specific significance of that sample.*

Not sure we understand this comment. This hierarchy in fact aims to help readers to follow the presentation of the data. Possibly we could change a (sub)heading.

- *Where is the thermodynamic modelling approach. How it was calculated the Effective Bulk Rock chemistry of each garnet overgrowing stage.*

See our summary statement: A summary of the approach will be added to the revised manuscript. Note that the effective bulk composition is part of the optimization function to be able to predict fractionation or resorption (see Fig. 3 and 4 in Lanari et al. 2017)

- *Discussion have to be rewrite to better focus the aims of the paper, taking into account previous or potential different interpretations, supporting the present one with more consistence.*

The revised Discussion will take this suggestion into account (in line with the comments of Referee #1).

- *The shape of the bounday for the study area identification not seem to be the same of the Fig. b.*

The shape of the study area is not exactly the same in the two maps due to graphic reasons and the big difference in the map scales, nonetheless it is representative

- *What is c*

Mistake corrected

- *To thick*

Ok, reduced

- *This image should be better emphasized with the use of the principal compoent analysis*

See our previous reply to the specific comment on "*Principal Component Analysis*"

- *These images should be better emphasized with the use of the principal compoent analysis*

See our previous reply to the specific comment on "*Principal Component Analysis*"

- *This figure look very good*

Thanks

We thank G. Ortolano-Referee #2 for his constructive comments.

Francesco Giuntoli, Pierre Lanari, Martin Engi

Deeply subducted continental fragments: I. Fracturing, dissolution-precipitation and diffusion processes recorded by garnet textures of the central Sesia Zone (Western Italian Alps)

Francesco Giuntoli[1], Pierre Lanari[1], Martin Engi[1]

[1]Institute of Geological Sciences, University of Bern, Baltzerstrasse 1+3, 3012 CH-Bern

Correspondence to: Francesco Giuntoli (francesco.giuntoli@plymouth.ac.uk)

Abstract. Contiguous continental high-pressure terranes in orogens offer insight into deep recycling and transformation processes that occur in subduction zones. These remain poorly understood, and currently debated ideas need testing. The approach we chose is to investigate in detail the record in suitable rocks samples that preserve textures and robust mineral assemblages, which withstood overprinting during exhumation. We document complex garnet zoning in eclogitic micaschists from the Sesia Zone (Western Italian Alps). These retain evidence of two orogenic cycles and provide detailed insight into resorption, growth and diffusion processes induced by fluid pulses at high pressure conditions. We analysed local textures and garnet compositional patterns, which turned out remarkably complex. By combining these with thermodynamic modelling, we could unravel and quantify repeated fluid-rock interaction processes. Garnet shows low-Ca porphyroclastic cores that were stable at (Permian) granulite facies conditions. The series of rims that surround these cores provides insight into the subsequent evolution: The first garnet rim that surrounds the pre-Alpine granulite facies core in one sample indicates that pre-Alpine amphibolite facies metamorphism followed the granulite facies event. In all samples documented, cores show lobate edges and preserve inner fractures, which are sealed by high-Ca garnet that reflect Alpine high-pressure conditions. These observations suggest that during early stages of subduction, before hydration of the granulites, brittle failure of garnet occurred, indicating high strain rates which may be due to seismic failure. Several Alpine rims show conspicuous textures indicative of interaction with hydrous fluid: (a) resorption-dominated textures produced lobate edges, at the expense of the outer part of the granulite core; (b) peninsulas and atoll garnet are the result of replacement reactions; (c) spatially limited resorption and enhanced transport of elements due the fluid phase is evident along brittle fractures and in their immediate proximity. Thermodynamic modelling shows that all of these Alpine rims formed at eclogite facies conditions. Structurally controlled samples allow these fluid-garnet interaction phenomena to be traced across a portion of the Sesia Zone, with a general decrease in fluid-garnet interaction observed towards the external, structurally lower parts of the terrane. Replacement of the Permian HT assemblages by hydrate-rich Alpine assemblages can reach nearly 100% of the rock volume. Since we found no clear relationship between discrete deformation structures (e.g. shear zones) observed in the field and the fluid pulses that triggered the transformation to eclogite facies assemblages, we conclude that disperse fluid flow was responsible for the hydration.

1 Introduction

Unravelling the metamorphic and deformational history in polyorogenic complexes is challenging, as relics from previous stages commonly were partially or completely overprinted during the subsequent stages. Garnet is a robust and common mineral frequently used to decipher metamorphic processes. It grows in a wide range of P-T conditions and rock types (e.g. Spear et al., 1984;O'Brien, 1997).

However, various processes may alter zoning recorded by garnet, notably replacement reactions and intracrystalline diffusion. Replacement of garnet may alter or completely obliterate garnet growth zones due to dissolution and reprecipitation processes (Putnis, 2002, 2009;Putnis and John, 2010;Ague and Axler, 2016). Relics will show resorption features, e.g. lobate or peninsular structures within a garnet growth zone, and sharp transitions in composition may be observed (e.g. Cruz, 2011). If the entire centre of a garnet is replaced by other mineral, typical atoll garnet may form (Atherton and Edmunds, 1966;Cooper, 1972;Smellie, 1974;Homam, 2003;Cheng et al., 2007;Faryad et al., 2010;Cruz, 2011;Ortolano et al., 2014a). Dissolution of garnet is thought to be linked to the presence of a (reactive) fluid, and may be followed by precipitation of new garnet with a different composition (Hames and Menard, 1993;Compagnoni and Hirajima, 2001;Cheng et al., 2007;Faryad et al., 2010;Wassmann and Stöckhert, 2013;Ortolano et al., 2014a;Ague and Axler, 2016). Diffusivity depends on temperature, time, and garnet composition, being generally higher for Fe^{2+}, Mg and Mn than for Ca (Carlson, 2006). Intracrystalline diffusion is relatively slow up to 700°C (e.g. Yardley, 1977;Spear, 1991;Carlson and Gordon, 2004;Caddick et al., 2010;Ague and Carlson, 2013): Below 700°C, garnet of a few hundred micrometres radius will retain compositional zoning for several tens of million years (Florence and Spear, 1991;Caddick et al., 2010).

Reconstructing the polyorogenic history stored in garnet requires an understanding of both texture and compositional zoning. To unravel the information recorded by garnet, we combined high-resolution electron probe compositional mapping with forward thermodynamic modelling. Our models account for fractional crystallisation and garnet resorption (Lanari et al., 2017). We applied this approach to several samples collected from the Internal Complex (as defined in Giuntoli and Engi, 2016) of the Sesia Zone, where garnet retains information from two orogenic cycles at very different conditions: Permian high-temperature followed by Alpine high-pressure (details in the next section).

We show that the textural and compositional changes are related to processes of dissolution, growth and diffusion. We discuss quantitative pressure (P) and temperature (T) information of garnet growth zones (data from Lanari et al., 2017; Giuntoli et al., in review) in relation with the observed textures. We propose that repeated local resorption and growth of garnet account for the complexly zoned garnets with lobate textures, peninsular features and, in the most extreme cases, formation of atoll garnet. Localized intracrystalline diffusion is observed only in the proximity of fractures, which were probably acting as main fluid pathways. For a series of four samples collected 2 kilometres across the main foliation and 5 kilometres along strike of the Internal Complex of the Sesia Zone, we infer that these garnet resorption and replacement processes are related to repeated fluid-rock interaction.

2 Geological setting and previous work on garnet

The Alpine orogenic belt formed between the Cretaceous and the Oligocene as a result of the convergence of the European plate and the Adriatic plate (Dewey et al., 1989;Rosenbaum et al., 2002;Handy et al., 2010). The Sesia Zone is a major high-pressure continental terrane located in the Italian Western Alps (Fig. 1a). It is thought to derive from the distal portion of the Adriatic passive margin that was involved in the Alpine subduction (Dal Piaz, 1999;Beltrando et al., 2014). The Sesia Zone is bounded to the west by blueschist to eclogite facies subunits derived from the Piemontese-Liguria Ocean (Bearth, 1967;Dal Piaz and Ernst, 1978;Martin et al., 1994;Cartwright and Barnicoat, 2002;Bucher et al., 2005;Groppo et al., 2009;Rebay et al., 2012;Negro et al., 2013) and to the east by the Insubric Line. This dextral brittle fault separates the Sesia Zone from the Southern Alps, which show a weak Alpine imprint at sub-greenschist facies (Bertolani, 1959;Zingg, 1983).

In the Aosta Valley (Fig. 1b) the Sesia Zone comprises two main complexes, i.e. the Internal and External Complexes (IC and EC hereafter; Giuntoli and Engi, 2016), separated by a greenschist facies shear zone. The EC comprises three epidote blueschist facies sheets of orthogneiss, with only minor paragneiss and metasediments, which are separated by lenses and bands, classically named Seconda Zona Diorito-Kinzigitica (2DK; Artini and Melzi, 1900;Dal Piaz et al., 1971;Compagnoni et al., 1977); these retain a pre-Alpine high-temperature imprint and only local evidence of the Alpine HP-history. The IC consists of several eclogitic subunits, each 0.5–3 km thick, separated by presumed monometamorphic (Mesozoic) meta-sediments (Venturini et al., 1994;Regis et al., 2014;Giuntoli and Engi, 2016). This complex is characterized by interlayered micaschist, eclogite, ortho- and paragneiss, with a very minor portion of pre-Alpine marbles and Mesozoic metasedimentary bands (e.g. Compagnoni, 1977;Castelli, 1991). The IC experienced eclogite facies conditions during Alpine metamorphism, with maximum recorded pressure of 2 GPa and temperature of 650-670 °C, between 85 and 55 Ma (Compagnoni, 1977;Konrad-Schmolke et al., 2011;Rubatto et al., 2011;Regis et al., 2014). Minor and local retrograde blueschist and greenschist facies overprints are present, especially close to tectonic contacts (Babist et al., 2006;Giuntoli and Engi, 2016). The IC preserves rare relics of pre-Alpine (Permian) granulite facies conditions (0.6-0.9GPa, ~850°C) and very sparse retrograde amphibolite facies conditions (0.5-0.3 GPa, 570-670°C; Lardeaux and Spalla, 1991;Rebay and Spalla, 2001;Zucali et al., 2002).

Polymetamorphic pre-Alpine garnet has been recognized in the IC since the works of Martinotti (1970), Compagnoni (1977), Zucali et al. (2002), and Robyr et al. (2014). This type of garnet shows coarse, optically bright pre-Alpine porphyroclasts, which are generally mantled by a rim of Alpine garnet with a dusty appearance due to inclusions. Alpine garnet is also present as smaller euhedral crystals. During greenschist-facies Alpine retrogression, garnet grains were partially retrogressed to chlorite, especially along grain boundaries and fractures. Robyr et al. (2014) found that the garnet texture depends on the matrix: Garnet forms mushroom- and atoll-shaped crystals in quartz-rich layers, but large idioblastic crystals in mica-rich layers. Four growth zones were identified, the first three of which were modelled as stable during prograde pre-Alpine Barrovian metamorphism from 500 to 600°C and 0.6 to 0.9 GPa. The fourth zone was modelled as stable at 550°C and 1.7-2.2 GPa, hence it is certainly Alpine in age, as pre-Alpine metamorphism had not reached eclogite facies conditions. Similar

garnet zoning was interpreted differently by Konrad-Schmolke et al. (2006) who concluded that the zones do not reflect two orogenic cycles, but are related to different water contents of the protoliths during Alpine HP subduction. In water-saturated rocks garnet would then display typical prograde zoning; whereas in water-undersaturated rocks garnet would produce more complex zoning, including abrupt compositional changes from core to rim.

3 Analytical methods

Numerous thin sections were studied by optical microscopy to characterize the structural and metamorphic relations among the main mineral phases. Backscattered electron (BSE) images were obtained using a Zeiss EVO50 scanning electron microscope at the Institute of Geological Sciences, University of Bern, using an accelerating voltage from 15 to 25 keV, a beam current of 500 pA, and a working distance of 10 mm.

Electron probe micro-analyses (EPMA) were performed using a JEOL JXA-8200 superprobe at the Institute of Geological Sciences, University of Bern. For compositional mapping, the procedure of Lanari et al. (2013) was used. Spot analyses were measured for each mineral phase present in the area of the maps before the maps were acquired. The investigated areas were mapped in wavelength-dispersive mode (WDS), with point analyses serving as internal standards. For point analyses, the analytical conditions were 15 KeV accelerating voltage, 20 nA specimen current, 40 s dwell times (including 2×10 s of background measurement), and ~1 µm beam diameter. Nine oxide compositions were analysed, using synthetic and natural standards: wollastonite/almandine (SiO_2), almandine (Al_2O_3), anorthite (CaO), almandine (FeO), spinel (MgO), orthoclase (K_2O), albite (Na_2O), ilmenite (TiO_2), and tephroite (MnO). For X-ray maps, analytical conditions were 15 KeV accelerating voltage, 100 nA specimen current, dwell times of 150-250 ms, and step sizes from 3 to 5 µm. Nine elements (Si, Ti, Al, Fe, Mn, Mg, Na, Ca and K) were measured at the specific wavelength in two passes. Intensity maps were standardized using spot analyses as internal standards. X-ray maps were classified and standardized using XMAPTOOLS 2.2.1 (Lanari et al., 2014). Structural formulae and end-member proportion maps were generated using the external functions provided in XMAPTOOLS. The following garnet end-members were used: Grossular ($Ca_3Al_2Si_3O_{12}$), Almandine ($Fe_3Al_2Si_3O_{12}$), Pyrope ($Mg_3Al_2Si_3O_{12}$), Spessartine ($Mn_3Al_2Si_3O_{12}$). Major element compositions were analysed by X-ray fluorescence (XRF) spectrometry at the University of Lausanne (Switzerland). Representative amounts of the samples were crushed and then pulverized in a tungsten carbide mill. The powder was dried for two hours at 105°C. Loss of ignition was then determined by weight difference after heating to 1050°C for 3 hours.

4 Sample selection strategy and petrography

The samples investigated are pelitic micaschists of the IC of the Sesia Zone displaying pale orange to greyish weathering surfaces. Grain sizes range from sub-millimetric to a few centimetres, with garnet in all samples showing either a single or bimodal size range. In this paper the term large grains refers to garnet several millimetres in diameter, small grains are 50-

200 µm in diameter. In plane-polarized transmitted light large garnet shows a clear core surrounded by a first rim that is dark due to finely dispersed inclusions, mostly of rutile needles (5-20 µm; Fig. 2, 3). Adjacent to this cloudy rim, some garnet grains show a clear outermost rim. The same core-rim structure is visible in BSE images, in which the core is brighter than the rims (e.g. Fig. 6a). In detail, garnet shows slightly different textures and compositions in each sample; petrographic and microstructural characteristics are summarized below and in Table 1.

These petrographic features match observations reported by previous authors (see section 2) who attempted to distinguish Alpine from pre-Alpine garnet in the Sesia Zone. Based on these observations, the sample selection strategy we adopted in this study used the following criteria:

- The presence in hand-specimens of garnet of diverse sizes (sub-millimetric to a few centimetres);
- A bimodal distribution of garnet in the same thin section, with the larger crystals displaying a bright core and dark rims and smaller euhedral crystals (Fig. 2);
- Bright cores surrounded by darker rims visible in the SEM with a BSE detector (e.g. Fig. 6a).

This list of criteria was adopted to investigate the widest possible range of microtextures and processes recorded by garnet. Applying the criteria lead us to concentrate on only ~5% of all the samples taken, mostly because larger (pre-Alpine) garnet grains rarely survived in the area we studied. In fact, almost all of the pre-Alpine HT assemblages had re-equilibrated in hydrate-rich Alpine assemblages.

Four of the samples used were from internal parts (South East - FG1315 and FG12157) and external parts (North West- FG1249 and FG1347) of the IC (Fig. 1b). Major element compositions for the samples are shown in the Supplement Table S1. FG1315 is a garnet white mica schist with a pervasive foliation marked by phengite, paragonite and allanite (Fig. S1). It shows a banding of quartz-rich and mica-rich layers. A stretching lineation, marked by mica and quartz, is well visible in the field and was confirmed by optical microscopy: Quartz shows a crystallographic preferred orientation. Allanite grains are elongate in the main foliation; they show a rim of clinozoisite up to 20 µm thick; rare monazite relics are preserved in the core. Rutile, graphite and zircons are present as accessory phases. Garnet displays two different micro-textures: (a) large crystals preserve a porphyroclastic core plus overgrowth zones, and (b) atoll garnet a few hundred microns in size. Where the garnet core is preserved, it is optically clear and shows inclusions of rutile containing rare ilmenite relics. The first garnet rim appears cloudy due to finely dispersed rutile inclusions, the outer rim is clear with few and coarser rutile inclusions (Fig. S5b). Both rims contain abundant quartz inclusions. Atoll garnet is optically clear; its core is now mainly composed of quartz and sparse phengite. Brittle fractures in both garnet types are lined by minor late chlorite. Locally, chlorite, albite and clinozoisite mark limited greenschist retrogression.

FG12157 is a glaucophane garnet micaschist. Its foliation is deformed by open folds and marked by phengite, glaucophane, and allanite (Fig. S2). Microscopically, glaucophane shows two growth zones, with lighter cores and darker blue pleochroic rims due to higher Fe-content. Some crystals are also rimmed by green Ca-amphibole. Allanite shows a rim of clinozoisite, up to 20 µm thick. Chlorite, albite and green amphibole mark greenschist retrogression. Accessory phases are graphite, zircon, and rutile; the latter has a titanite overgrowth followed by an ilmenite rim. Garnet is present as large grains with a

clear core with several quartz inclusions at the periphery. The first garnet rim (Rim1) is dark, due to fine sagenitic rutile inclusions, locally as needles with a 120° intersection that may mark dissolved Ti-rich biotite. The second garnet rim (Rim2) is more clear (Fig. 3). Glaucophane and phengite locally occur within Rim1 or between Rim1 and Rim2. Apatite inclusions are presents in the core and both rims.

FG1249 is a rutile garnet micaschist with phengite, paragonite, allanite, and rutile defining an intense foliation that wraps around garnet of several millimetres size (Fig. S3). Allanite occurs rimmed by epidote; monazite is a rare relic in allanite cores. Sparse glaucophane is partly overgrown by albite and green amphibole. Garnet shows an optically clear core and a dark rim due to finely dispersed rutile (µm size) and paragonite inclusions. Coarser rutile (up to 100 µm) is included in the core as well as are phengite and apatite; paragonite and quartz are concentrated at the core-rim transition. Some chlorite fractures dissect entirely the garnet grains. Chlorite, albite, epidote, and green amphibole also reflect limited greenschist retrogression.

FG1347 is a chloritoid garnet micaschist with a strong foliation marked by phengite, chloritoid, paragonite, allanite and rutile that wraps around large garnet porphyroblasts. (Fig. S4). In the field an intense stretching lineation is marked by chloritoid. Microscopically, chloritoid is found in two generations, the younger of which is poikiloblastic and overgrows the main foliation. Accessory phases are zircon and opaque minerals. Some hundred microns monazite grains are preserved and are partially overgrown by allanite and apatite symplectites; allanite is rimmed by clinozoisite. Chlorite grew at the expense of the garnet rim and along brittle fractures. Garnet is several millimetres in size, with a clear core and a dark rim full of fine rutile inclusions, as in the other samples. Quartz inclusions are abundant in the rim (Fig. S6b).

5 Results

5.1 Evolution of successive garnet stages

High-resolution X-ray maps were helpful to study garnet microtextures, because element distributions were well visible and allowed us to investigate patterns that will be demonstrated to reflect growth and dissolution processes. The complex geometry of end-member proportion maps reveals several zones of distinct composition (Figs. 3-4) surrounding the garnet core, which are neither visible by optical microscopy nor in backscatter electron images. While some geometric variability is evident among individual grains and from one sample to another, certain prominent features are consistently observed in most of them. Maps of grossular fraction (X_{Grs}, Fig. 4) provide the clearest distinction of growth zones and are most suitable to identify similarities among all the samples. Generally, maps of the almandine and pyrope fractions provide patterns similar to grossular (except in one sample, FG1249, discussed below). The common feature evident in X_{Grs} maps of all samples is a core poor in Ca, containing fractures sealed by a more calcic garnet. The core is surrounded by several rims, all of them with higher X_{Grs} (Fig. 4), but subtle differences exist between the rims of each specimen, as discussed in the following sections.

Two types of fractures are visible: (i) millimeter-long fractures dissect entire garnet grains; these late fractures (Fig. 3c) are lined by chlorite; (ii) micrometer-thin cracks, visible only in compositional maps, form a fracture network in garnet cores; these so-called inner fractures were sealed by garnet richer in grossular (Fig. 3c; Fig. 4). Average compositions of garnet growth zones are reported in Table 2.

5.1.1 FG1315

The X_{Grs} map shows a porphyroclastic core of uniform composition ($Alm_{68}Prp_{27}Grs_{4}Sps_{1}$), with lobate edges and a dense network of inner fractures sealed by more calcic garnet ($Alm_{67}Prp_{23}Grs_{9}Sps_{1}$; Figs. 4a, S5). Rim1 surrounds the rounded relic core and is higher in grossular content ($Alm_{60}Prp_{20}Grs_{19}Sps_{1}$) that the core; Rim1 is thinner in the direction of the main foliation, peninsular growth of Rim1 extends into the core. Rim2 ($Alm_{64}Prp_{24}Grs_{11}Sps_{1}$) is found as three textural types: (a) It grew externally onto Rim1; (b) between core and Rim1, and also surrounds the Rim1 peninsula, thus extending it (by ~20 µm); (c) fine veins (5-20 µm thick) dissecting Rim1 also show Rim2 composition (as discussed in section 6.2). The outermost rim (Rim3) is lower in grossular ($Alm_{69}Prp_{24}Grs_{6}Sps_{1}$); it displays peninsular growths inside Rim1 and Rim2. Remarkably, Rim3 is thin (~100 µm) parallel to the main foliation and thicker (~400 µm) perpendicular to it. Zoning patterns in atoll garnet (Fig. 5) are analogous, as are the grossular contents. The inner growth surfaces of Rim1 define negative garnet crystal forms, whereas Rim2 overgrowths are present on the outside growth surface only. Rim3 is the outermost growth zone, with peninsulas that formed at the expense of the previous rims.

5.1.2 FG12157

Garnet cores are chemically zoned, with domains showing high spessartine and pyrope contents but relatively low almandine fractions (Fig. 6; zoning profile of the garnet end-member in Fig. 2 of Lanari et al., 2017). The porphyroclastic core (average composition: $Alm_{69}Prp_{25}Grs_{4}Sps_{2}$) shows lobate edges and is fractured, but cracks are sealed by more calcic garnet ($Alm_{66}Prp_{21}Grs_{12}Sps_{1}$; Figs. 3c, 4b, 6c). Three overgrowth zones surround the core: Rim1 is higher in grossular ($Alm_{63}Prp_{20}Grs_{16}Sps_{1}$) than the core; Rim2 is higher yet ($Alm_{59}Prp_{17}Grs_{23}Sps_{1}$) and grew both internally and externally of Rim1. Rim3 is present just locally as the outermost rim ($Alm_{64}Prp_{20}Grs_{15}Sps_{1}$).

5.1.3 FG1249

A core and three rim generations are evident in the compositional maps (Fig. 7; zoning profile in Fig. 8). As in the other samples, the core is lowest in grossular ($Alm_{72}Prp_{18}Grs_{5}Sps_{5}$) and shows a fracture pattern, which was sealed by garnet with higher grossular contents ($Alm_{60}Prp_{18}Grs_{20}Sps_{2}$; Figs. 4c, 7c). Compared to the core, Rim1 is higher in grossular ($Alm_{75}Prp_{15}Grs_{9}Sps_{1}$) and its outer edge is euhedral. Rim2 is higher in grossular than the previous growth zone ($Alm_{62}Prp_{20}Grs_{17}Sps_{1}$) and quite similar to the fracture fillings. It is variable in thickness, but present both at the core-Rim1 boundary and peripheral to Rim1. Rim3 is the outermost growth zone and highest in grossular ($Alm_{58}Prp_{18}Grs_{23}Sps_{1}$). Its thickness varies, giving the entire garnet a euhedral shape. Locally, Rim3 is present also at the core-Rim1 boundary (Fig. 8).

This zoning pattern shows different features along the main fracture zones and around them: A sharp and strong decrease in Alm and Sps and increase in Prp contents are visible. Rim 1, 2 and 3 are also found in small garnet crystals (ø 0.1-0.5 mm) in which no core is visible.

5.1.4 FG1347

The core is zoned, with patchy areas high in X_{Sps} and X_{Alm} but low in X_{Prp} (Fig. S6). The X_{Grs} map (Fig. 4d) reveals a dense fracture pattern in the core ($Alm_{68}Prp_{27}Grs_{3}Sps_{2}$) sealed by more calcic garnet ($Alm_{68}Prp_{25}Grs_{6}Sps_{1}$). These fractures stop immediately against Rim1, which is highest in grossular content ($Alm_{66}Prp_{22}Grs_{11}Sps_{1}$). Rim2 ($Alm_{67}Prp_{26}Grs_{6}Sps_{1}$) is strongly asymmetric: It is wider perpendicular to the main foliation, as are Rim3 ($Alm_{69}Prp_{26}Grs_{4}Sps_{1}$) and Rim4 ($Alm_{71}Prp_{25}Grs_{3}Sps_{1}$). Additionally, clasts of Rim2, Rim3 and Rim4 are partly dismembered from the main garnet crystal, indicating deformation, which we note to be conspicuously absent in the other samples.

5.2 Modeling phase equilibria in partially re-equilibrated rocks

Several garnet growth zones were identified in each sample by detailed analysis of the end-member proportion maps using XMAPTOOLS (Lanari et al., 2014). Representative areas were selected and their average garnet composition extracted. Such areas are chemically homogeneous and uniform amongst different garnet grains, they display no evidence of enrichment or depletion in major elements. The quantitative micro-mapping strategy employed in this study has well established advantages (e.g. Marmo et al., 2002;Lanari et al., 2013;Ortolano et al., 2014b;Angiboust et al., 2016) over traditional spot analyses: (1) it allows key relationships, such as the successive growth zones, to be identified and relevant compositions to be constrained, (2) it permits testing if chemical zoning patterns are consistent over several grains, which helps support (or refute) the assumption of grain boundary equilibrium (e.g. Lanari and Engi, 2017), (3) it can be used to approximate local reactive bulk composition by accounting for (non-reactive) mineral relics. In all the samples of the present study, growth zone patterns and compositions of the mineral phases were consistent at thin section scale.

The complexity of garnet compositional zoning shown in Figures 4, 5, 6, 7 indicates that isochemical phase diagrams (or pseudosections) must be used with due caution. Previous studies have demonstrated that garnet fractionation potentially affects the reactive bulk composition (Evans, 2004;Robyr et al., 2014;Konrad-Schmolke et al., 2008) and thus shifts the calculated garnet isopleths in a P-T diagram (Lanari and Engi, 2017). However, garnet fractionation is not easy to account for where several growth stages are evident, as well as intermittent dissolution (which we show to be the case in the companion paper by Giuntoli et al., in review). Since the older growth zones are but partially preserved, as indicated e.g. by lobate edges (Figs. 3, 4, 6, 7) in our samples, a specific modelling strategy was developed and implemented in a computer program (GRTMOD: Lanari et al., 2017). In essence, for each garnet growth zone, the reactive bulk composition is optimized jointly with the P-T conditions to predict (using Theriak-Domino, de Capitani and Petrakakis, 2010) a garnet composition that matched the measured one. Results were accepted if the residual value (the least square sum of the differences) between the modelled and observed garnet compositions (end-member fractions) was <0.05, reflecting a close match. Previously

formed garnet generations were removed from the bulk rock composition, based on the analysis of end-member proportion maps. By analogy, in the case of garnet resorption, the appropriate components were again added to the reactive bulk composition. This iterative modeling approach was applied to each successive growth zone. The resulting P-T estimates are reported in Figure 9b, with error bars showing the P-T uncertainty related to the analytical error of the garnet composition (Lanari et al., 2017). For any given reactive bulk composition, narrowly spaced isopleths return small uncertainty envelopes, whereas widely spread isopleths return larger ones. A detailed description of these methods is presented in the companion paper (Giuntoli et al., in review).

5.3 Results of thermodynamic modelling of garnet growth zones

PT estimates obtained from the garnet growth zones are summarized here with the main purpose of distinguishing between pre-Alpine (HT) and Alpine (HP) growth periods. The full dataset used is provided and discussed in more detail in Giuntoli et al. (in review). Figure 9 summarizes the composition of all the garnet growth zones in a ternary diagram (Alm, Prp, Grs) and the optimal P-T conditions determined for each growth zone. Notably, in each sample studied the crystals analysed in thin section all show the same chemical zoning pattern.

Some preliminary remarks are needed here before presenting the detailed results for each sample. Garnet cores in all modelled samples indicate growth at granulite facies conditions (Fig. 9). In sample FG1249 only the garnet core shows an overgrowth (Rim1) for which modelling indicates amphibolite facies conditions (Fig. 9). Rim1 in this sample is considered to be pre-Alpine, since amphibolite to granulite facies conditions are well established to be upper Paleozoic (Kunz et al., 2017) in the terrane sampled, i.e. the central Sesia Zone. HT conditions at low to intermediate pressures have never been reported for the Alpine metamorphism, which is of eclogite facies grade. Indeed, all other garnet rims in the samples studied indicate eclogite facies conditions, hence are attributed to the Alpine cycle. This is in line with the HP mineral inclusions of phengite, glaucophane and rutile (see section 4; Figs. 5b, 6b, 7b, S5b, S6b) in garnet, as well as our results of P-T modelling (Fig. 9). The sealed inner fractures did not require special consideration in modelling because of their low modal abundance («1 volume %). However, we note that their composition matches that of Alpine rims (e.g. Rim2 in sample FG1315). Conditions found from one sample to the next show minor differences, indicating spatial and/or temporal gradients in the P-T conditions. Given that the terrane sampled contains several tectonic slices (Giuntoli and Engi, 2016), it is certainly possible that these conditions may not have been recorded in all samples at the same time of the evolution of the belt.

FG1315: The garnet core is predicted at ~0.8 GPa and 750 °C. The HP Alpine rims are modelled at ~1.5 GPa and 650°C, 1.9 GPa and 650°C, 1.8 GPa and 670°C respectively.

FG12157: Modelling indicates ~0.6 GPa and 900 °C for the core; Alpine Rim1 and Rim2 are predicted at ~1.6 GPa, 650°C and ~1.4 GPa, 630°C, respectively.

FG1249: The pre-Alpine core is modelled at ~0.6 GPa and 730°C; 10 vol% of garnet core is predicted to have crystallized (Fig. 10). Rim1 grew at pre-Alpine amphibolite facies conditions (~0.6 GPa and 620°C); GrtMod predicted resorption of 2 % of the core and growth of 2 % Rim1. Alpine Rim2 crystallized at ~1.6 GPa, 620°C; the model yields 10 vol% growth of

Rim2 and less than 1 % resorption of previous generations. Rim3 crystallized at ~1.5 GPa, 660°C with 7 % resorption of garnet Rim2 and growth of 9 % Rim3.

FG1347: The pre-Alpine core is modelled stable at ~0.8 GPa and 770°C. All Alpine rims (1-3) are modelled stable between 1.7-2.0 GPa and 580-600°C.

6 Discussion

As summarized in the previous section, garnet cores are modelled stable in granulite facies conditions; Rim1 of sample FG1249 suggests amphibolite facies conditions. In situ U-Pb dating of metamorphic growth rims in zircon from all the samples presented in this study gave lower Permian weighted mean ages (~295-280 Ma; results presented in Kunz et al., 2017). These data are in agreement with the late Permian retrograde metamorphism from granulite to amphibolite facies conditions proposed by Lardeaux and Spalla (1991) and Rebay and Spalla (2001). Except for Rim1 in FG1249, all of the garnet rims modelled are found to be stable at eclogite facies conditions that are similar to those recently determined for the central Sesia Zone (e.g. Konrad-Schmolke et al., 2006;Konrad-Schmolke and Halama, 2014;Regis et al., 2014;Rubatto et al., 2011;Lanari et al., 2017). In the following, the main textures recognized in garnet are discussed and related to specific processes.

6.1 Micrometre-size fracture network in garnet cores

A network of fine fractures is present in all of the pre-Alpine cores of the samples (inner fractures in Fig. 3c; Fig. 4). These fractures have widths from few microns to some tens of microns and irregular shapes, with sharp edges and conjugate systems with 90° interception. These fractures are not localized around inclusions and do not show a radial distribution, so inclusion-induced fracturing during decompression is ruled out as a mechanism of formation (e.g. Whitney, 1996;Wendt et al., 1993). The fractures are not visible by optical or scanning electron microscopy, as they are sealed by a garnet similar in composition to the first HP Alpine generations. These small-scale fillings are considered coeval with the formation of one of the first Alpine garnet rims, as they are similar in chemical composition.

In outer parts of the core fractures are less abundant, and the more calcic garnet sealed cracks show sharp boundaries against the old garnet core composition. In central parts the core appears “cloudy”, owing to the dense network of sealed cracks, so the finely spaced sealed cracks are more difficult to discriminate. Minor diffusional smoothing may have occurred over a scale up to ten microns. In the present samples, the fracture network in garnet cores is best observed in the X_{Grs} maps, but is also evident in other X-ray maps, notably of Fe and Mg, but less so for Mn (except for FG1249), possibly because the concentration is too low to detect such a small variation in Mn. Grossular fraction has long been known to be strongly pressure-dependent (Kretz, 1959), and pressure is the physical variable expected to vary particularly in a subduction setting. Moreover, Ca in garnet is among the divalent elements least affected by diffusion up to fairly high temperature (e.g. Carlson 2006), so it is most likely to retain growth features.

The network of cracks observed in our samples probably reflects brittle deformation of garnet, which implies a small ductility contrast between garnet and the matrix (e.g. Raimbourg et al., 2007). High strain rates that induced these cracks may well have been related to seismic failure (Austrheim and Boundy, 1994;Austrheim et al., 1996;Austrheim et al., 2017;Angiboust et al., 2012;Wang and Ji, 1999;Hertgen et al., 2017). Note that pervasive deformation, e.g. by shearing, would have dismembered the fractured garnet cores, which is not observed. Since the mineral assemblages formed by Permian granulite facies metamorphism were mostly anhydrous, the rheological contrast between garnet and its matrix is expected to have been small, up to the HP Alpine (re)hydration (Engi et al., in review). As we show in the following, fractures in a rheologically strong mineral like garnet and their subsequent sealing thus provide a link from the Permian HT- to the Cretaceous HP-conditions, more specifically related to the first stage of fluid influx (Fig. 10a). Apart from such fractures in the garnet cores, pre-Alpine or other pre-eclogite facies fabrics are but rarely preserved in the study area because Alpine metamorphic re-equilibration at eclogite facies conditions can reach nearly 100% (see also section 6.4). Specifically, the brittle stages visible at micron scale in garnet cores could not be directly linked to any locally or regionally prevalent strain patterns.

Nevertheless, we cannot rule out that some of the fractures developed in pre-Alpine time, notably in an extensional tectonic setting. This has been proposed for other localities (Floess and Baumgartner, 2013), where garnet breakdown occurred at LT and LP, involving a volume increase and hydration. However, in the present case, micrometer-wide fractures dissect pre-Alpine garnet, and the coherence of these fractured grains is preserved. We found no chemical evidence of any LT- or LP-alteration predating the growth of Ca-enriched garnet, except for one sample (FG1249, discussed below). All these observations indicate an Alpine origin for the fracture network and suggest that these were healed by a new garnet generation before the fragments were dismembered by subsequent strain. Most probably the formation of fractures and growth of garnet inside these fractures were closely related, and mineral compositions indicate that this occurred at eclogite facies conditions. Moreover, comparable garnet textures in a similar geological context (Mt. Emilius klippe) have been interpreted to reflect fracturing and sealing at Alpine eclogite facies conditions (Pennacchioni, 1996;Hertgen et al., 2017;Angiboust et al., 2016)

Brittle behavior of garnet is also manifested during the retrograde Alpine greenschist facies conditions (0.15-0.3 GPa and 300-350°C) in other samples from the IC of the Sesia Zone. This deformative stage produced textures varying from fragmented garnet, showing no displacement, to trails and pods of garnet (several hundred microns in size) that represent torn-apart garnet porphyroclasts (Trepmann and Stöckhert, 2002;Küster and Stöckhert, 1999). Such fractures cut through all the garnet growth zones (Fig. 4 in Trepmann and Stöckhert, 2002), these are not healed by garnet, instead chlorite frequently crystallized along them. Fractures in garnet are filled by retrograde metamorphic minerals (e.g. chlorite, feldspar, epidote) if they form out of the stability field of garnet (e.g. Prior, 1993). Based on these criteria, we suggest such a mechanism for the millimeter-long fractures (named late fractures in Fig. 3c, see section 5.1) we found in our samples. These cut through all the garnet generations and are completely different from the fine fractures discussed above.

6.2 Resorption and growth: fluid-related textures

Our samples record several stages of resorption with unequal portions of garnet being affected (Fig. 4). Resorption is most extensive in sample FG1315, as judged by textures: Lobate edges, peninsular structures, veins inside Rim1, and formation of atoll garnet (Figs. 4a, 5, 10b, S5). In particular, the vein network dissects Rim1, and resorption is evident along these veins and on both sides of Rim1, prior to growth of Rim2. Note that Rim2 displays the same chemical composition in all of these domains. For this reason, we surmise that Rim1 and 2 are not a simple growth sequence, with the older, internal generation being overgrown more externally by a younger rim. Instead, the geometry indicates that the older growth zone (Rim1) was partially resorbed and replaced by a younger one (Rim2) that precipitated on both sides of Rim1. This interpretation is also supported by numerous micrometre-size rutile inclusions in Rim1; these highlight paleo-porosity, an essential feature of the replacement processes (e.g. Putnis, 2015). Analogous zoning patterns are evident also in samples FG12157 and FG1249 Rim1 and 2, even though the vein network in these samples is less clearly visible in the compositional maps.

Four processes have been proposed to account for the formation of atoll garnet: (a) simultaneous multiple nucleation and coalescence processes (e.g. Cooper, 1972;Spiess et al., 2001), (b) rapid and short-term poikiloblastic growth (e.g. Atherton and Edmunds, 1966;Ushakova and Usova, 1990), (c) changes in the stoichiometry of the garnet-forming reaction (Robyr et al., 2014), and (d) dissolution of the core that was rendered unstable (by changes P-T conditions), and precipitation of new garnet stable in the presence of circulating fluid (e.g. Smellie, 1974;Homam, 2003;Cheng et al., 2007;Faryad et al., 2010;Ortolano et al., 2014a). In sample FG1315 textures in large garnet cores (up to several mm in size) reflect partial resorption, showing lobate structures or peninsular features. Detailed thermodynamic modelling of this sample (Giuntoli et al., in review) predicts extensive resorption of garnet cores during the formation of Rim3. Based on this evidence, we conclude that atoll garnet formation was related to process (d), i.e. partial dissolution of the unstable HT-core under HP-conditions in the presence of a fluid. Note that the effect of this process is grain size-dependent, and atoll garnet cores observed in this sample are indeed limited in size from 50 to a few hundred microns. So, while destabilization of these small garnets lead to complete replacement of the core, the latter was not entirely replaced in the large garnets (Fig. 10b). In FG1315, resorption textures are also visible in the Permian growth zone of zircon, as documented by Giuntoli et al. (in review). Resorption occurred at several stages, as evident from the peninsulas in which garnet Rim1 crystallized and was successively enlarged by Rim2 and by Rim3. Figure 10b summarizes the growth / resorption chronology of garnet in this sample.

Resorption and growth textures in sample FG12157 are similar to those in FG1315, except that no atoll garnet is observed. However, a drastically different type of textural features is found in sample FG1249: Neither clear lobate structures nor peninsulas indicate resorption, except for a narrow Rim2 that grew at the expense of garnet core and Rim1. The growth chronology of the sample FG1249 is summarized in Fig. 10a. In sample FG1347, resorption traces are limited close to the fracture network in the core, with minor resorption of Rim2 (Fig. 4d).

With one exception, all of the samples presented above also contain zircon and sparse monazite; these are only preserved as pre-Alpine (Permian) relics in the core of Alpine allanite. The exception is FG12157 where monazite is completely pseudomorphed by allanite and apatite; (Giuntoli et al., in review). Apart from garnet and these accessory relics, the main pre-Alpine HT assemblage has completely re-equilibrated at eclogite facies conditions. This is also evident from the volatile contents of these samples and their high percentages of hydrous minerals: LOI (loss-on-ignition) values range from 1.58% to 2.44% (Table S1) compared to values of 0.5-0.7 wt% for proposed equivalent rocks in the Ivrea Zone, i.e. pre-Alpine upper amphibolite to granulite facies samples lacking an Alpine facies overprint (Engi et al., in review). As detailed in that study, this implies that the nominally dry pre-Alpine HT assemblages were replaced in response to disperse infiltration of hydrous fluid. This Alpine hydration process occurred in several pulses or stages (Fig. 10). Previous partial hydration is evident only in one sample (FG1249), in which a first rim formed during pre-Alpine retrogression from granulite to amphibolite facies conditions. In all other cases studied, the increase in bulk rock volatile contents happened during the Alpine HP-evolution, when fluid was imported while the IC was in the subduction channel. This hydration is expected to have enhanced ductile deformation and metamorphic reaction rates (Austrheim, 1990;Austrheim et al., 1997;Pennacchioni, 1996).

6.3 Re-equilibration close to fluid pathways

As described in section 5.1.3, fractures in the pre-Alpine garnet cores are evident in X-ray maps made from sample FG1249, and all garnet end member maps show that these are sealed by garnet of a composition ($Alm_{62}Prp_{18}Grs_{18}Sps_2$) similar to the two Alpine rims (Rim2 and Rim3). Note that the core is chemically uniform, as expected in granulite facies garnet owing to fast diffusion at high temperature (e.g. Caddick et al., 2010). However, in an area some 500 µm wide (indicated by white arrows in Fig. 7), garnet is affected by fractures, and the $X_{Alm,\ Prp,\ Sps}$ maps show that it is compositionally different from the core, except for a few islands where original granulite facies garnet remains, and it displays an Alpine composition (Figs. 7, 8). This feature is best observed in the Mn-map, which serves as a marker delimiting the original pre-Alpine garnet core with its high X_{Sps} values (0.05-0.06; Fig. 7f). Overprinted areas show a sharp decrease in X_{Sps}, down to values of 0.02. The X_{Grs} map (Fig. 7c) is drastically different, as garnet displays the same composition as pristine pre-Alpine generations (X_{Grs} 0.05 and 0.09 for core and Rim1, respectively), except just a few microns away from the fractures.

This zoning pattern suggests that fractures provided fluid access, initiating a re-equilibration process that affected the surrounding volume of garnet over a distance of several hundred microns. As minor fractures are visible branching from the major ones, we consider this area as a damaged zone in which re-equilibration of the garnet was enhanced along a network of micro-fractures and in their proximity, due to the increased area/volume ratio (Austrheim et al., 1996;Pennacchioni, 1996). Erambert and Austrheim (1993) reported similar fracture patterns in pre-Caledonian granulite garnet of the Bergen Arcs (Western Norway), and they interpret these as fluid channels along which element mobility was enhanced. These studies concluded that re-equilibration of granulite-facies garnet during Caledonian eclogite conditions occurred proportionally to the fracture density and fluid availability.

In the present samples, re-equilibration processes affecting garnet were evidently much more effective for Alm, Prp, and Sps than for Grs. We propose that diffusion of Ca ions through the damaged lattice of the original garnet was slower than of Fe^{2+}, Mg, and Mn. Conspicuously similar phenomena were observed by Erambert and Austrheim (1993). Their evidence is in line with what we discussed above, i.e. that new garnet formed just along fractures; in neighbouring areas strong overprinting of original garnet is observed for Prp, Alm and Sps but not for Grs. Raimbourg et al. (2007) advanced that intra- and inter-granular transport of Ca in garnet is inefficient compared to Fe^{2+} and Mg. Volume diffusion of divalent ions is slow in garnet at temperatures below 700 °C (Ganguly, 2010), but differences in interdiffusion between Ca, Mg, Fe, and Mn are notable (e.g. Carlson, 2006).

In the latest phases of this re-equilibration process, brittle fractures would have been sealed by the Alpine garnet visible along the fracture walls. This may have occurred in several stages, as can be inferred from the X_{Grs} map, where garnet sealing the fractures has the composition of Rim2 and Rim3 (Figs. 7, 8).

X_{Sps} can be used as a tracer of re-equilibration processes also in samples where the effect of such processes on garnet texture it is not as striking as for FG1249. This is the case in samples FG12157 and FG1347, in which high fracture density in the core corresponds with low spessartine values (Figs. 6f, S6f). Furthermore, zoning found in the core of FG1347 for Alm, Prp and Sps is not evident in the X_{Grs} map, again indicating that re-equilibration in the proximity of the main fluid pathways was more effective for Fe^{2+}, Mg, and Mn than for Ca ions.

6.4 Hydration through the IC

The previous sections used garnet textures linked to the main paragenesis and P-T modelling results from Giuntoli et al. (in review) to show that the IC of the central Sesia Zone in the Aosta Valley underwent pre-Alpine granulite facies metamorphism with local amphibolite facies retrogression, followed by major Alpine hydration occurring at different stages of the eclogite facies evolution. As discussed in the previous sections, garnet textures suggest a decrease in the amount of fluid-garnet interaction and related pervasive resorption features from internal areas (South East - FG1315 and FG12157) to external area (North West - FG1249 and FG1347) of the IC (Fig. 1b). Such a tendency is supported by field observation (Giuntoli and Engi, 2016), as the only mesoscopic boudin of pre-Alpine amphibolites found in the area of the IC studied (Compagnoni, 1977) is located close to sample FG1347. These amphibolites are only partially re-equilibrated at eclogite facies conditions, and they preserve pre-Alpine hornblende and plagioclase (Compagnoni, 1977;Gosso et al., 2010).

Hydration in internal areas (SE parts) of the IC started during early subduction metamorphism, as recorded by prograde lawsonite (Zucali and Spalla, 2011) and continued up to the highest P-T conditions recorded in the present samples. In external (NW) areas of the IC a second generation of lawsonite provides evidence of hydration occurring right after rocks reached their HP climax, when temperature decreased (Pognante, 1989). This stage was related to H_2O-rich (low XCO_2) fluids possibly along preferential channels, producing metasomatism, as reflected by local occurrences of lawsonite in high modal amounts (up to 60 vol.-%).

In the central Sesia Zone (mainly in an area south of the Aosta Valley, whereas our samples were taken north of it), Konrad-Schmolke et al. (2006) found evidence that micaschists similar to those reported here also were not fully hydrated prior to Alpine subduction. Based on P-T modelling, that study concluded that extensive influx of hydrous fluid would have been required for these rocks to remain water-saturated between 1.2 and 1.8 GPa. This is similar to our results, but Konrad-Schmolke et al. (2011) invoked open-system pervasive fluid flow in the Tallorno Shear Zone and concluded that hydration occurred at retrograde blueschist conditions, at the expense of eclogite-facies felsic and basic rocks. They suggest that the minimum amount of fluid interacting with the wall-rocks was 0.1-0.5 wt%. In our samples, a retrograde hydration is significant in only one sample (FG12157), for which P-T modelling indicates a second fluid influx at 1.4 GPa and 650°C (Rim2). In addition, several samples in the area we studied do show minor amounts of hydration during retrograde greenschist facies, but these effects are local and minor (<5% retrogression in most samples). A strong greenschist overprint (replacing 50-90% of the eclogite parageneses) is limited to the vicinity of the major tectonic contact between the IC and EC (Barmet Shear Zone; Giuntoli and Engi, 2016). By analogy, we surmise that the hydration stage described by Konrad-Schmolke et al. (2011) is a relatively late phenomenon occurring in a confined area during retrograde blueschist conditions, whereas the main hydration of the Internal Complex in the region of Aosta Valley occurred during the prograde P-T trajectory, at eclogite facies conditions, as described in this study. The timing of fluid infiltration is reflected by Alpine allanite and zircon ages (Regis et al., 2014;Rubatto et al., 2011;Giuntoli, 2016;Giuntoli et al., in review) and reflects a heterochronous evolution in several tectonic sheets, with older ages (85-77 Ma) generally in the internal (SE) areas of the IC, and younger ages (72-55 Ma) towards external areas (NW).

While textural and chemical evidence indicates that external fluid repeatedly interacted with initially nearly dry protoliths at HP conditions, we have no tight constraints on how much fluid entered at what spatial or temporal intervals. However, for each growth stage (within any one sample), the composition of garnet produced is uniform in each grain analysed, whereas their local geometry differs to some extent. This allows a spatial estimate of the reaction volume involved: Interaction of hydrous fluid with the reactive part of the assemblage (i.e. the matrix minerals) must have been at the scale of a thin section (centimetres) at least, except that incomplete reaction progress left garnet relics. Apart from garnet and local accessories (zircon, monazite), no mineral relics of the successive replacement reactions have been detected, indeed these rocks appear otherwise fully equilibrated at eclogite facies conditions.

Unlike in the Norwegian Caledonides, the relationships between deformation structures that acted as fluid pathways (e.g. Austrheim, 1987) is not clearly evident in our samples. Eclogitization of pre-Alpine granulites and amphibolites in the IC seems to be more an effect of pervasive but disperse fluid infiltration, not of channelized flow. At the microscale sample FG1249 may be considered an exception, since it shows tracks of more channelized fluid flow preserved in millimetric garnets.

In Western Norway, lithological heterogeneities do not seem to play a major role in the localization of deformation, whereas detailed mapping shows that the Internal Complex of the Sesia Zone consists of a pile of tectonic sheets, a few kilometres in thickness (Giuntoli and Engi, 2016). These sheets show internal lithological heterogeneity, with micaschist, eclogites, minor

para- and orthogneiss interlayered at scales from a few millimetres to about a hundred metres. The rheological contrasts among these different rock bodies might well have been where small-scale shear bands nucleated, which served as conduits for fluid infiltration (Oliver, 1996).

7 Conclusions

This study documents complexly zoned garnet in polyorogenic rocks that were extensively deformed and (re)hydrated during Alpine eclogite facies metamorphism. Garnet in pelitic schists commonly preserves a porphyroclastic core that reflects medium-pressure HT-metamorphism. These granulite facies conditions prevailed during the Permian and converted the sedimentary protoliths to mostly anhydrous assemblages, which are rarely preserved in the area studied. In the sample suite reported here, pre-Alpine conditions are evident just in garnet cores and relic zircon (Kunz et al., 2017). The relic features show brittle deformation textures, i.e. cracks, but no displacement. These textures reflect high strain rates at the onset of Alpine tectonics, and they may have been generated by seismic failure. In garnet, a network of micrometre-size fractures crosscut the core (and locally a first Alpine overgrowth), and these cracks were sealed by new generations of garnet. Their composition is more calcic and corresponds to the Alpine HP-rims of garnet.

The interaction of percolating fluid with garnet repeatedly produced resorption features, such as lobate structures, peninsulas, or atoll garnet. Textures indicating limited resorption are less common. In rocks where these features are present, re-equilibration produced by intracrystalline diffusion is located in close proximity to brittle fractures, which acted as fluid pathways. Re-equilibration of Mg, Fe and Mn due to diffusion enhanced by fluid occurred over distances of several hundred micrometres, while Ca re-equilibrated over a much smaller distance (few micrometres), indicating slower diffusion. The intensity of prograde hydration and HP-overprinting, as reflected in the preserved garnet textures, varies among the samples analysed. The set as a whole indicates regional differences, as notably the fluid-garnet interaction intensity appears to a decrease (from SE to NW) over a few kilometres within the Internal Complex of the Sesia Zone. In some areas of the same complex, other studies found another phase of decompression-related (blueschist facies) hydration that appears to be related to a major shear zone. In most external (NW) parts of the Sesia zone studied here, a later, strong greenschist overprint is dominant.

This study shows that compositional (X-ray) maps linked with petrographic and microstructural analysis serve as powerful tools to document detailed mineral textures, particularly in garnet. When combined with thermodynamic modelling results, such images facilitate the analysis and permit quantification of local processes that act at (sub)grain scale, such as local growth and resorption, which play a critical role in hydrating HT protoliths and converting them to eclogite facies assemblages.

Data availability

Original data underlying the material presented care available by contacting the authors.

Competing interests.

The authors declare that they have no conflict of interest.

Acknowledgements

We thank Martin Robyr for his help in performing EMPA. Discussions with him and Jörg Hermann have been particularly fruitful. We acknowledge constructive comments and suggestions from Gaetano Ortolano and an anonymous referee. Patrice Rey is warmly thanked for editorial handling. This work was supported by the Swiss National Science Foundation (Project 200020-146175).

References

Ague, J. J., and Carlson, W. D.: Metamorphism as garnet sees it: the kinetics of nucleation and growth, equilibration, and diffusional relaxation, Elements, 9, 439-445, 2013.

Ague, J. J., and Axler, J. A.: Interface coupled dissolution-reprecipitation in garnet from subducted granulites and ultrahigh-pressure rocks revealed by phosphorous, sodium, and titanium zonation, Am. Mineral., 101, 1696-1699, 2016.

Angiboust, S., Agard, P., Yamato, P., and Raimbourg, H.: Eclogite breccias in a subducted ophiolite: A record of intermediate-depth earthquakes?, Geology, 40, 707-710, 2012.

Angiboust, S., Yamato, P., Hertgen, S., Hyppolito, T., Bebout, G., and Morales, L.: Fluid pathways and high pressure metasomatism in a subducted continental slice (Mt. Emilius klippe, W. Alps), J. Metamorph. Geol., 2016.

Artini, E., and Melzi, G.: Ricerche petrografiche e geologiche sulla Valsesia, Tipografia Bernardoni di C. Rebeschini, 1900.

Atherton, M., and Edmunds, W.: An electron microprobe study of some zoned garnets from metamorphic rocks, Earth Planet. Sci. Lett., 1, 185-193, 1966.

Austrheim, H.: Eclogitization of lower crustal granulites by fluid migration through shear zones, Earth Planet. Sci. Lett., 81, 221-232, 10.1016/0012-821X(87)90158-0, 1987.

Austrheim, H.: The granulite-eclogite facies transition: A comparison of experimental work and a natural occurrence in the Bergen Arcs, western Norway, Lithos, 25, 163–169, http://dx.doi.org/10.1016/0024-4937(90)90012-P, 1990.

Austrheim, H., and Boundy, T.: Pseudotachylytes generated during seismic faulting and eclogitization of the deep crust, Science, 265, 82-84, 1994.

Austrheim, H., Erambert, M., and Boundy, T. M.: Garnets recording deep crustal earthquakes, Earth Planet. Sci. Lett., 139, 223-238, 1996.

Austrheim, H., Erambert, M., and Engvik, A. K.: Processing of crust in the root of the Caledonian continental collision zone: the role of eclogitization, Tectonophysics, 273, 129-153, 1997.

Austrheim, H., Dunkel, K. G., Plümper, O., Ildefonse, B., Liu, Y., and Jamtveit, B.: Fragmentation of wall rock garnets during deep crustal earthquakes, Science Advances, 3, e1602067, 2017.

Babist, J., Handy, M. R., Hammerschmidt, K., and Konrad-Schmolke, M.: Precollisional, multistage exhumation of subducted continental crust: The Sesia Zone, western Alps, Tectonics, 25, 10.1029/2005TC001927, 2006.

Bearth, P.: Die Ophiolite der Zone von Zermatt-Saas Fee, Beiträge zur Geologischen Karte der Schweiz, 132, 130, 1967.

Beltrando, M., Manatschal, G., Mohn, G., Dal Piaz, G. V., Brovarone, A. V., and Masini, E.: Recognizing remnants of magma-poor rifted margins in high-pressure orogenic belts: The Alpine case study, Earth-Science Reviews, 131, 88-115, 2014.

Bertolani, M.: La formazione basica "Ivrea-Verbano" e la sua posizione nel quadro geologico-petrografico della bassa Val Sesia e del Biellese, Periodico di Mineralogia, 28, 151-209, 1959.

Bucher, K., Fazis, Y., Capitani, C. D., and Grapes, R.: Blueschists, eclogites, and decompression assemblages of the Zermatt-Saas ophiolite: High-pressure metamorphism of subducted Tethys lithosphere, Am. Mineral., 90, 821-835, 2005.

Caddick, M. J., Konopásek, J., and Thompson, A. B.: Preservation of garnet growth zoning and the duration of prograde metamorphism, J. Petrol., 51, 2327-2347, 2010.

Carlson, R. W., and Gordon, C. L.: Effects of matrix grain size on the kinetics of intergranular diffusion, J. Metamorph. Geol., 22, 733-742, 2004.

Carlson, W. D.: Dana Lecture. Rates of Fe, Mg, Mn, and Ca diffusion in garnet, Am. Mineral., 91, 1-11, 2006.

Cartwright, I., and Barnicoat, A.: Petrology, geochronology, and tectonics of shear zones in the Zermatt–Saas and Combin zones of the Western Alps, J. Metamorph. Geol., 20, 263-281, 2002.

Castelli, D.: Eclogitic metarmophism in carbonate rocks: the example of impure marbles from the Sesia-Lanzo Zone, Italian Western Alps, J. metamorphic Geol., 9, 61-77, 1991.

Cheng, A., Nakamura, E., Kobayashi, K., and Zhou, Z.: Origin of atoll garnets in eclogites and implications for the redistribution of trace elements during slab exhumation in a continental subduction zone, Am. Mineral., 92, 1119-1129, 2007.

Compagnoni, R.: The Sesia-Lanzo Zone: high pressure-low temperature metamorphism in the Austroalpine continental margin, Rend. Soc. Ital. Mineral. Petrol., 33, 335-375, 1977.

Compagnoni, R., Dal Piaz, G., Hunziker, J., Gosso, G., Lombardo, B., and Williams, P.: The Sesia-Lanzo Zone, a slice of continental crust with Alpine high pressure-low temperature assemblages in the Western Italian Alps, Rend. Soc. Ital. Mineral. Petrol, 33, 281-334, 1977.

Compagnoni, R., and Hirajima, T.: Superzoned garnets in the coesite-bearing Brossasco-Isasca Unit, Dora-Maira massif, Western Alps, and the origin of the whiteschists, Lithos, 57, 219-236, 2001.

Cooper, A.: Progressive metamorphism of metabasic rocks from the Haast Schist Group of southern New Zealand, J. Petrol., 13, 457-492, 1972.

Cruz, M. D. R.: Origin of atoll garnet in schists from the Alpujárride Complex (Central zone of the Betic Cordillera, Spain): Implications on the PT evolution, Mineral. Petrol., 101, 245-261, 2011.

Dal Piaz, G. V., Gosso, G., and Martinotti, G.: La II Zona Diorito-Kinzigitica tra la Valle Sesia e la Valle d'Ayas (Alpi Occidentali), Memorie della Società Geologica Italiana, 11, 433–460, 1971.

Dal Piaz, G. V., and Ernst, W. G.: Areal geology and petrology of eclogites and associated metabasalts of the Piemonte ophiolite nappe, Breuil-St. Jaques area, Italian Western Alps, Tectonophysics, 51, 99-126, 1978.

Dal Piaz, G. V.: The Austroalpine-Piedmont nappe stack and the puzzle of the Alpine Tethys, Mem. Sci. Geol., 51, 155-176, 1999.

de Capitani, C., and Petrakakis, K.: The computation of equilibrium assemblage diagrams with Theriak/Domino software, Am. Mineral., 95, 1006-1016, 10.2138/am.2010.3354, 2010.

Dewey, J., Helman, M., Knott, S., Turco, E., and Hutton, D.: Kinematics of the western Mediterranean, Geological Society, London, Special Publications, 45, 265-283, 1989.

Engi, M., Giuntoli, F., Lanari, P., Burn, M., Kunz, B. E., and Bouvier, A.-S.: Pervasive eclogitization due to brittle deformation and rehydration of subducted basement. Effects on continental recycling?, Geochemistry, Geophysics, Geosystems (G^3), in review.

Erambert, M., and Austrheim, H.: The effect of fluid and deformation on zoning and inclusion patterns in poly-metamorphic garnets, Contrib. Mineral. Petrol., 115, 204-214, 1993.

Evans, T. P.: A method for calculating effective bulk composition modification due to crystal fractionation in garnet-bearing schist; implications for isopleth thermobarometry J. Metamorph. Geol., 22, 547-557, 2004.

Faryad, S., Klápová, H., and Nosál, L.: Mechanism of formation of atoll garnet during high-pressure metamorphism, Mineral. Mag., 74, 111-126, 2010.

Floess, D., and Baumgartner, L.: Formation of garnet clusters during polyphase metamorphism, Terra Nova, 25, 144-150, 2013.

Florence, F. P., and Spear, F. S.: Effects of diffusional modification of garnet growth zoning on PT path calculations, Contrib. Mineral. Petrol., 107, 487-500, 1991.

Ganguly, J.: Cation diffusion kinetics in aluminosilicate garnets and geological applications, Rev. Mineral. Geochem., 72, 559-601, 2010.

Giuntoli, F.: Assembly of continental fragments during subduction at HP: Metamorphic history of the central Sesia Zone (NW Alps), PhD thesis, University of Bern, Switzerland, 2016.

Giuntoli, F., and Engi, M.: Internal geometry of the central Sesia Zone (Aosta Valley, Italy): HP tectonic assembly of continental slices, Swiss J. Geosci., 109, 445-471, 2016.

Giuntoli, F., Lanari, P., Burn, M., Kunz, B. E., and Engi, M.: Deeply subducted continental fragments: II. Insight from petrochronology in the central Sesia Zone (Western Italian Alps), Solid Earth, in review.

Gosso, G., Messiga, B., Rebay, G., and Spalla, M. I.: Interplay between deformation and metamorphism during eclogitization of amphibolites in the Sesia-Lanzo Zone of the Western Alps, Int. Geol. Rev., 52, 1193-1219, 2010.

Groppo, C., Beltrando, M., and Compagnoni, R.: The P–T path of the ultra-high pressure Lago di Cignana and adjoining high-pressure meta-ophiolitic units: insights into the evolution of the subducting Tethyan slab, J. Metamorph. Geol., 27, 207-231, 2009.

Hames, W., and Menard, T.: Fluid-assisted modification of garnet composition along rims, cracks, and mineral inclusion boundaries in samples of amphibolite facies schists, Am. Mineral., 78, 338-344, 1993.

Handy, M. R., Schmid, S. M., Bousquet, R., Kissling, E., and Bernoulli, D.: Reconciling plate-tectonic reconstructions of Alpine Tethys with the geological–geophysical record of spreading and subduction in the Alps, Earth-Science Reviews, 102, 121-158, 2010.

Hertgen, S., Yamato, P., Morales, L. F., and Angiboust, S.: Evidence for brittle deformation events at eclogite-facies PT conditions (example of the Mt. Emilius klippe, Western Alps), Tectonophysics, 706, 1-13, 2017.

Homam, S. M.: Formation of atoll garnet in the Ardara Aureole, NW Ireland, Journal of Sciences Islamic Republic of Iran, 14, 247-258, 2003.

Konrad-Schmolke, M., Babist, J., Handy, M. R., and O'Brien, P. J.: The physico-chemical properties of a subducted slab from garnet zonation patterns (Sesia Zone, Western Alps), J. Petrol., 47, 2123-2148, 2006.

Konrad-Schmolke, M., O'Brien, P. J., De Capitani, C., and Carswell, D. A.: Garnet growth at high- and ultra-high pressure conditions and the effect of element fractionation on mineral modes and composition, Lithos, 103, 309-332, 2008.

Konrad-Schmolke, M., O'Brien, P. J., and Zack, T.: Fluid migration above a subducted slab – Constraints on amount, pathways and major element mobility from partially overprinted eclogite-facies rocks (Sesia Zone, Western Alps), J. Petrol., 52, 457-486, 10.1093/petrology/egq087, 2011.

Konrad-Schmolke, M., and Halama, R.: Combined thermodynamic–geochemical modeling in metamorphic geology: Boron as tracer of fluid–rock interaction, Lithos, 208, 393-414, 2014.

Kretz, R.: Chemical study of garnet, biotite and hornblende from gneisses of S.W. Quebec, with emphases on distribution of elements in coexisting minerals, Journal of Geology, 67, 371-402, 10.1086/626594, 1959.

Kunz, B. E., Manzotti, P., von Niederhäusern, B., Engi, M., Darling, J. R., Giuntoli, F., and Lanari, P.: Permian high-temperature metamorphism in the Western Alps (NW Italy), Int. J. Earth Sci., 1-27, 10.1007/s00531-017-1485-6, 2017.

Küster, M., and Stöckhert, B.: High differential stress and sublithostatic pore fluid pressure in the ductile regime—microstructural evidence for short-term post-seismic creep in the Sesia Zone, Western Alps, Tectonophysics, 303, 263-277, 1999.

Lanari, P., Riel, N., Guillot, S., Vidal, O., Schwartz, S., Pêcher, A., and Hattori, K. H.: Deciphering high-pressure metamorphism in collisional context using microprobe mapping methods: Application to the Stak eclogitic massif (northwest Himalaya), Geology, 41, 111-114, 2013.

Lanari, P., Vidal, O., Lewin, E., Dubacq, B., De Andrade, V., and Schwartz, S.: XMapTools a Matlab©-based graphic user interface for microprobe quantified image processing, Computers and Geosciences, 62, 227-240, 10.1016/j.cageo.2013.08.010, 2014.

Lanari, P., and Engi, M.: Local Bulk Composition Effects on Metamorphic Mineral Assemblages, Reviews in Mineralogy & Geochemistry, 83, 55–102, http://dx.doi.org/10.2138/rmg.2017.83.1, 2017.

Lanari, P., Giuntoli, F., Loury, C., Burn, M., and Engi, M.: An inverse modeling approach to obtain P-T conditions of metamorphic stages involving garnet growth and resorption, Eur. J. Mineral., 29, 181-199, 10.1127/ejm/2017/0029-2597, 2017.

Lardeaux, J. M., and Spalla, M. I.: From granulites to eclogites in the Sesia zone (Italian Western Alps): a record of the opening and closure of the Piedmont ocean, J. metamorphic Geol., 9, 35-59, 1991.

Manzotti, P., Ballevre, M., Zucali, M., Robyr, M., and Engi, M.: The tectonometamorphic evolution of the Sesia–Dent Blanche nappes (internal Western Alps): review and synthesis, Swiss J. Geosci., 107, 309-336, 2014.

Marmo, B., Clarke, G., and Powell, R.: Fractionation of bulk rock composition due to porphyroblast growth: effects on eclogite facies mineral equilibria, Pam Peninsula, New Caledonia, J. Metamorph. Geol., 20, 151-165, 2002.

Martin, S., Tartarotti, P., and Dal Piaz, G.: The Mesozoic ophiolites of the Alps: A review, Bollettino di Geofisica teorica ed applicata, 36, 1994.

Martinotti, G.: Studio petrografico delle eclogiti della zona del Monte Mucrone e dei loro rapporti con i "micascisti eclogitici" incassanti, Unpublished Thesis, Universita Torino, 1970.

Negro, F., Bousquet, R., Vils, F., Pellet, C.-M., and Hänggi-Schaub, J.: Thermal structure and metamorphic evolution of the Piemont-Ligurian metasediments in the northern Western Alps, Swiss J. Geosci., 106, 63-78, 2013.

O'Brien, P. J.: Garnet zoning and reaction textures in overprinted eclogites, Bohemian Massif, European Variscides: a record of their thermal history during exhumation, Lithos, 41, 119-133, 1997.

Oliver, N.: Review and classification of structural controls on fluid flow during regional metamorphism, J. Metamorph. Geol., 14, 477-492, 1996.

Ortolano, G., Visalli, R., Cirrincione, R., and Rebay, G.: PT-path reconstruction via unraveling of peculiar zoning pattern in atoll shaped garnets via image assisted analysis: an example from the Santa Lucia del Mela garnet micaschists (northeastern Sicily-Italy), Periodico di Mineralogia, 83, 257-297, 2014a.

Ortolano, G., Zappalà, L., and Mazzoleni, P.: X-Ray Map Analyser: A new ArcGIS® based tool for the quantitative statistical data handling of X-ray maps (Geo-and material-science applications), Comput. Geosci., 72, 49-64, 2014b.

Pennacchioni, G.: Progressive eclogitization under fluid-present conditions of pre-Alpine mafic granulites in the Austroalpine Mt Emilius Klippe (Italian western Alps), J. Struct. Geol., 18, 549-561, 1996.

Pognante, U.: Lawsonite, blueschist and eclogite formation in the southern Sesia zone (Western Alps, Italy), Eur. J. Mineral., 1, 89–104, 1989.

Prior, D. J.: Sub-critical fracture and associated retrogression of garnet during mylonitic deformation, Contrib. Mineral. Petrol., 113, 545-556, 1993.

Putnis, A.: Mineral replacement reactions: from macroscopic observations to microscopic mechanisms, Mineral. Mag., 66, 689-708, 2002.

Putnis, A.: Mineral replacement reactions, Rev. Mineral. Geochem., 70, 87-124, 2009.

Putnis, A., and John, T.: Replacement processes in the Earth's crust, Elements, 6, 159-164, 2010.

Putnis, A.: Transient porosity resulting from fluid–mineral interaction and its consequences, Rev. Mineral. Geochem., 80, 1-23, 2015.

Raimbourg, H., Goffé, B., and Jolivet, L.: Garnet reequilibration and growth in the eclogite facies and geodynamical evolution near peak metamorphic conditions, Contrib. Mineral. Petrol., 153, 1-28, 2007.

Rebay, G., and Spalla, M. I.: Emplacement at granulite facies conditions of the Sesia–Lanzo metagabbros: an early record of Permian riftig?, Lithos, 58, 85–104, 2001.

Rebay, G., Spalla, M. I., and Zanoni, D.: Interaction of deformation and metamorphism during subduction and exhumation of hydrated oceanic mantle: Insights from the Western Alps, J. Metamorph. Geol., 30, 687-702, 10.1111/j.1525-1314.2012.00990.x, 2012.

Regis, D., Rubatto, D., Darling, J., Cenki-Tok, B., Zucali, M., and Engi, M.: Multiple metamorphic stages within an eclogite-facies terrane (Sesia Zone, Western Alps) revealed by Th-U-Pb petrochronology, J. Petrol., 55, 1429-1456, 10.1093/petrology/egu029, 2014.

Robyr, M., Darbellay, B., and Baumgartner, L. P.: Matrix-dependent garnet growth in polymetamorphic rocks of the Sesia zone, Italian Alps, J. Metamorph. Geol., 32, 3-24, 2014.

Rosenbaum, G., Lister, G. S., and Duboz, C.: Relative motions of Africa, Iberia and Europe during Alpine orogeny, Tectonophysics, 359, 117-129, 2002.

Rubatto, D., Regis, D., Hermann, J., Boston, K., Engi, M., Beltrando, M., and McAlpine, S.: Yo-Yo subduction recorded by accessory minerals (Sesia Zone, Western Alps) Nat. Geosci., 4, 338-342, 10.1038/ngeo1124, 2011.

Smellie, J.: Formation of atoll garnets from the aureole of the Ardara pluton, Co. Donegal, Ireland, Mineral. Mag., 39, 878-888, 1974.

Spear, F.: On the interpretation of peak metamorphic temperatures in light of garnet diffusion during cooling, J. Metamorph. Geol., 9, 379-388, 1991.

Spear, F. S., Selverstone, J., Hickmott, D., Crowley, P., and Hodges, K.: PT paths from garnet zoning: A new technique for deciphering tectonic processes in crystalline terranes, Geology, 12, 87-90, 1984.

Spiess, R., Peruzzo, L., Prior, D., and Wheeler, J.: Development of garnet porphyroblasts by multiple nucleation, coalescence and boundary misorientation-driven rotations, J. Metamorph. Geol., 19, 269-290, 2001.

Trepmann, C. A., and Stöckhert, B.: Cataclastic deformation of garnet: a record of synseismic loading and postseismic creep, J. Struct. Geol., 24, 1845-1856, 2002.

Ushakova, E., and Usova, L.: Atoll garnets in the contact aureole of an area of southeastern Tuva, Geologia i Geofizika, 31, 50-59, 1990.

Venturini, G., Martinotti, G., Armando, G., Barbero, M., and Hunziker, J. C.: The Central Sesia–Lanzo Zone (Western Italian Alps): new field observations and lithostratigraphic subdivisions, Schweiz. Mineral. Petrogr. Mitt., 74, 111-121, 1994.

Wang, Z., and Ji, S.: Deformation of silicate garnets: Brittle-ductile transition and its geological implications, Can. Mineral., 37, 525-541, 1999.

Wassmann, S., and Stöckhert, B.: Low stress deformation of garnet by incongruent dissolution precipitation creep, J. Struct. Geol., 46, 200-219, 2013.

Wendt, A. S., D'Arco, P., Goffé, B., and Oberhänsli, R.: Radial cracks around α-quartz inclusions in almandine: constraints on the metamorphic history of the Oman Mountains, Earth Planet. Sci. Lett., 114, 449-461, 1993.

Whitney, D. L.: Garnets as open systems during regional metamorphism, Geology, 24, 147-150, 1996.

Whitney, D. L., and Evans, B. W.: Abbreviations for names of rock-forming minerals, Am. Mineral., 95, 185-187, 2010.

Yardley, B. W. D.: An empirical study of diffusion in garnet, Am. Mineral., 62, 793-800, 1977.

Zingg, A.: The Ivrea and Strona Ceneri Zones (Southern Alps, Ticino and Northern Italy): A review., Schweiz. Mineral. Petrogr. Mitt., 63, 361-392, 1983.

Zucali, M., Spalla, M. I., and Gosso, G.: Strain partitioning and fabric evolution as a correlation tool: the example of the Eclogitic Micaschists Complex in the Sesia–Lanzo Zone (Monte Mucrone–Monte Mars, Western Alps, Italy), Schweiz. Mineral. Petrogr. Mitt., 82, 429–454, 2002.

Zucali, M., and Spalla, M. I.: Prograde lawsonite during the flow of continental crust in the Alpine subduction: Strain vs. metamorphism partitioning, a field-analysis approach to infer tectonometamorphic evolutions (Sesia-Lanzo Zone, Western Italian Alps), J. Struct. Geol., 33, 381-398, 2011.

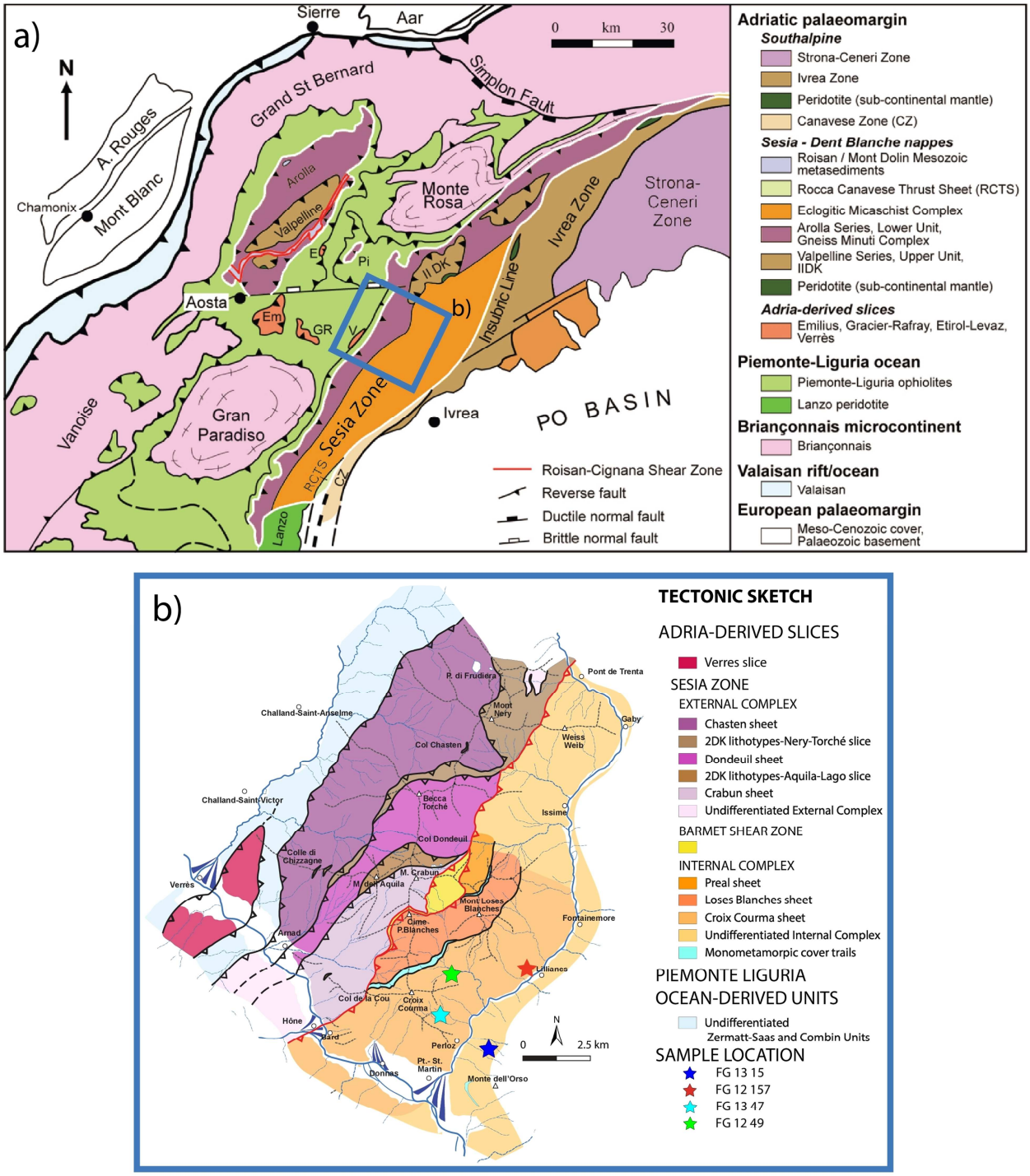

Figure 1: (a) Simplified tectonic map of the Western Alps (modified from Manzotti et al. (2014), location of study area. (b) Tectonic sketch of study area with sample locations (modified from Giuntoli and Engi, 2016).

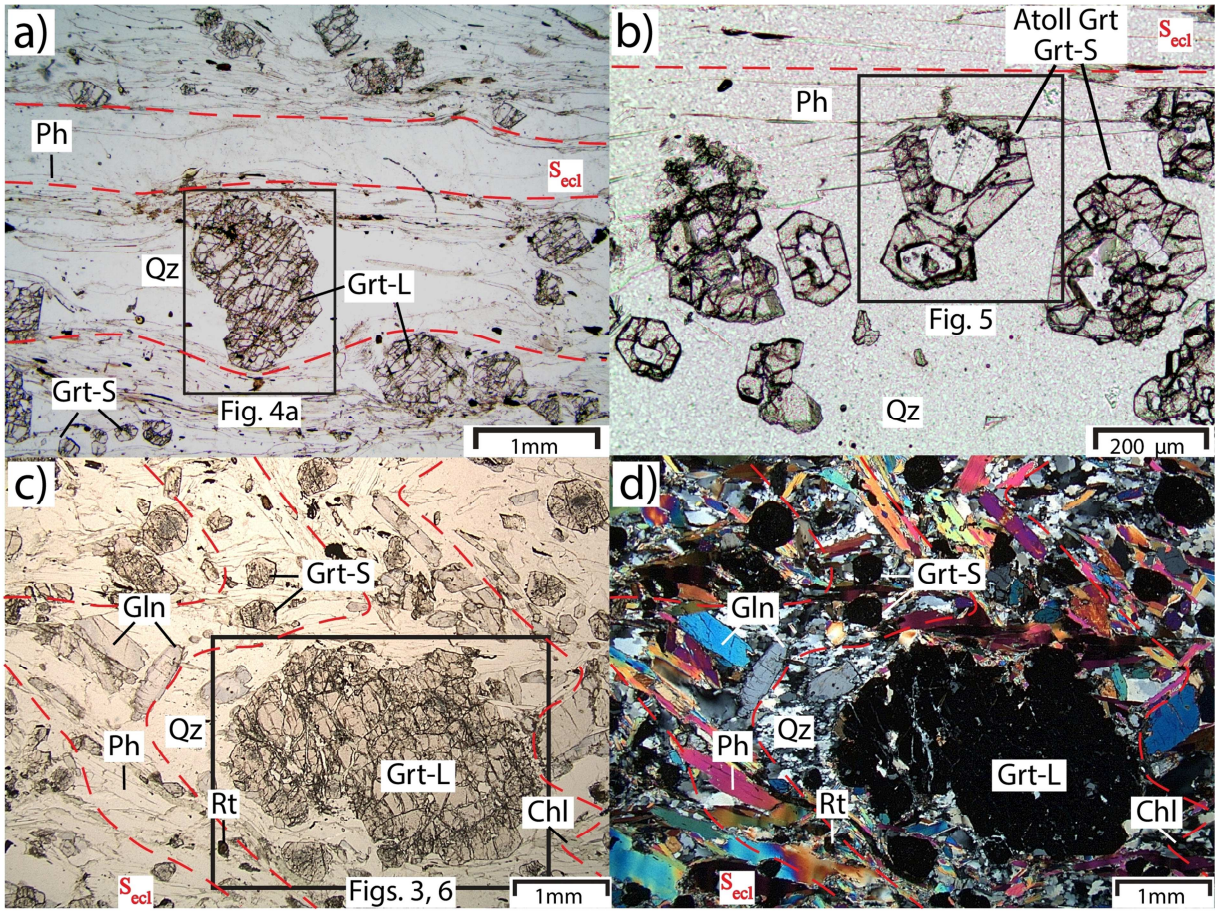

Figure 2: Thin section optical microphotos displaying the eclogitic foliation (S_{ecl}, red dashed line) and the bimodal size range of garnet (large garnet grains Grt-L; small garnet grains Grt-S; see text for further details). Black squares indicate the location of the high-resolution X-ray maps presented in the following figures. (a) S_{ecl} wrapping Grt-L grains in sample FG1315. (b) Same thin section as (a) with atoll garnets (Grt-S) located within a Qz rich band and a Ph rich band. (c) and (d) Folded S_{ecl} marked by Ph, Gln and Rt; Chl is present in the fold hinges. Plane-polarized light: (a, b, c); cross-polarized light (d).

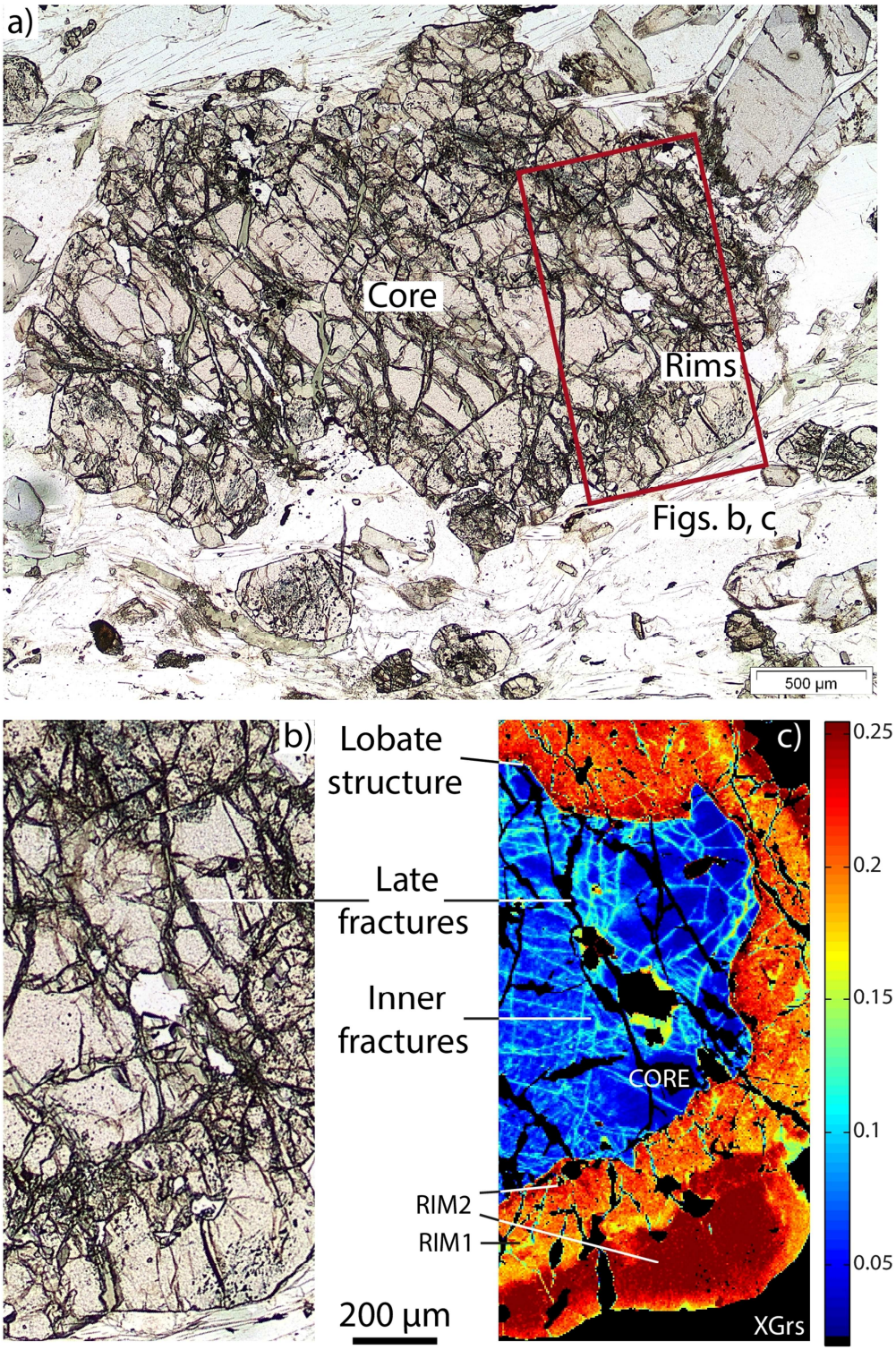
a)
Core
Rims
Figs. b, c
500 µm
b)
Lobate structure
Late fractures
Inner fractures
RIM2
RIM1
200 µm
c)
CORE
XGrs
0.25
0.2
0.15
0.1
0.05

Figure 3: Garnet porphyrocryst in FG12157, (a) and (b): Optical microphoto, plane polarized light. (a): Clear lobate core, dark inner rim, speckled with inclusions (mostly rutile, up to 20 µm long), outer rim more clear with only minor inclusions. (b) Enlargement shows later fractures (dark) that dissect the entire garnet and contain chlorite. c Grossular X-ray map; blue Ca-poor core reveals numerous micrometre-size fractures sealed by more calcic garnet; sparse late fractures (black) in core and rims. Compare to complete maps in Figs. 4b, 6.

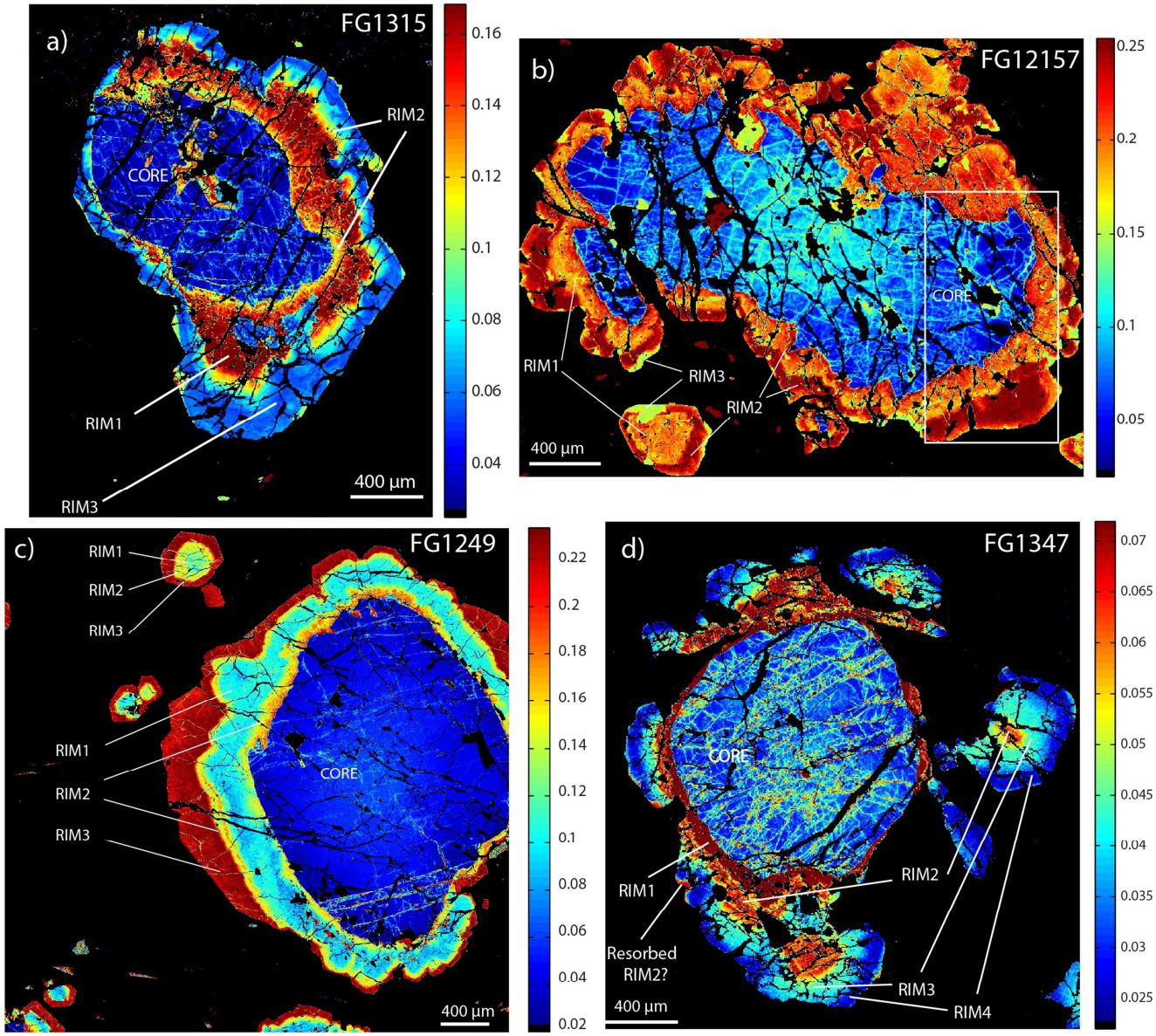

Figure 4: Growth zones visible in standardized X-ray maps for the grossular end-member. The foliation in all photos is horizontal. Note that a fractured core poor in X_{Grs} is present in all samples and always rimmed by several garnet growth zones. In FG1315 (a) and FG12157 (b) textures indicating resorption include lobate edges and peninsulas (the white rectangle indicates the location of Figs. 3b, c). In FG1249 (c) resorption is inferred from the growth of Rim2 both inside and outside Rim1. In FG1347 (d) resorption is limited to the fractures in the core and Rim2 (see text); rims vary in thickness in each generation of overgrowths.

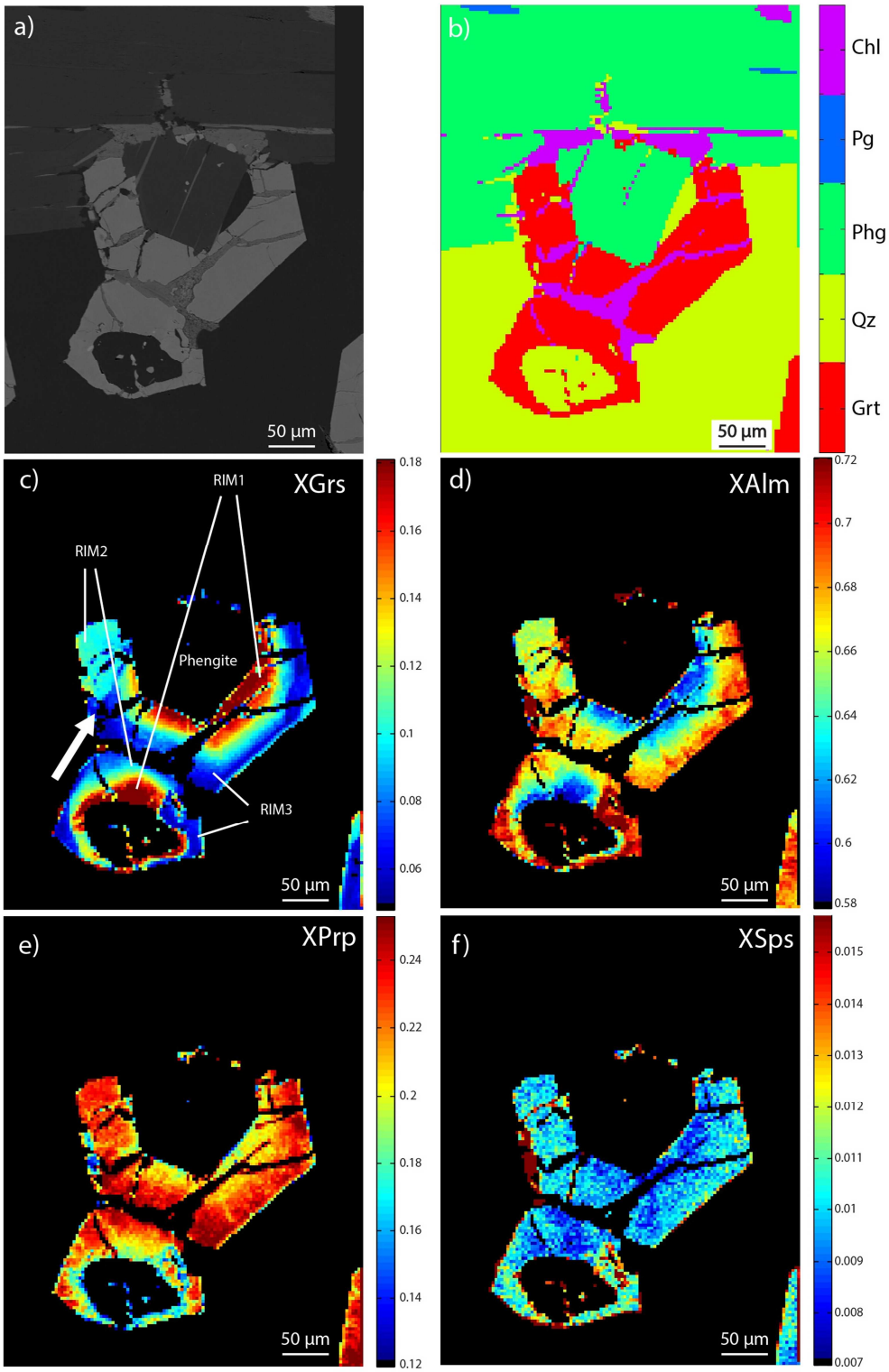
a)
50 µm
b)
50 µm
Chl
Pg
Phg
Qz
Grt
c)
XGrs
RIM1
RIM2
Phengite
RIM3
50 µm
0.18
0.16
0.14
0.12
0.1
0.08
0.06
d)
XAlm
50 µm
0.72
0.7
0.68
0.66
0.64
0.62
0.6
0.58
e)
XPrp
50 µm
0.24
0.22
0.2
0.18
0.16
0.14
0.12
f)
XSps
50 µm
0.015
0.014
0.013
0.012
0.011
0.01
0.009
0.008
0.007

Figure 5: Small atoll garnet (ø ~100 µm) in sample FG1315. (a) BSE picture. (b) Mineral phases (determined from X-ray maps). Note inclusions of quartz and phengite in the atoll core; fractures dissecting the entire garnet are filled by chlorite. Garnet occurs at the contact of quartz- and phengite-rich bands that define the main foliation. (c) Standardized X-ray map for the X_{Grs} end-member. Note the analogous zoning pattern as for large garnet (Fig. S5), with same X_{Grs} contents and a Rim3 peninsula extending into the resorbed rims (arrow). (d), (e), (f) Standardized X ray maps for X_{Alm}, X_{Prp}, and X_{Sps} respectively.

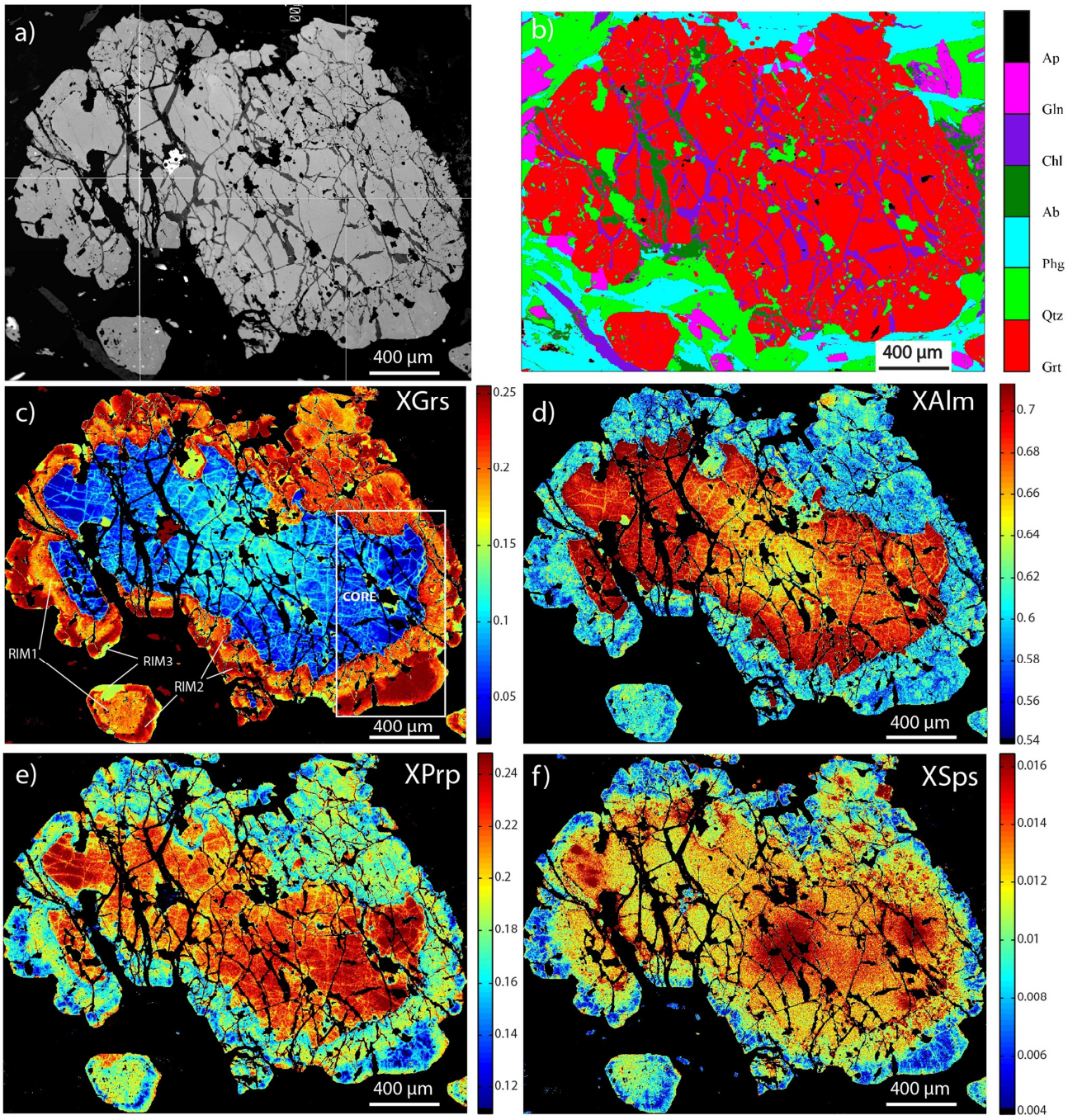

Figure 6: Large garnet (ø ~2-3 mm) in sample FG12157. (a) BSE picture with a bright porphyroclastic core and a darker rim. (b) Mineral phases (based on X-ray maps). Quartz inclusions are present in several garnet growth zones, but locally mark the core-Rim1 boundary; note that fractures (filled by chlorite and albite) dissect the entire garnet

grain. Glaucophane and phengite seem to be intergrown with garnet Rim2. (c) Standardized X-ray map for X_{Grs} end-member (the white rectangle indicates the location of Figs. 3b, c. Note the lobate edges along the core and the fracture network within the core that is sealed by garnet higher in X_{Grs}. Zoning patterns in small garnet crystals are similar. (d), (e) Standardized X-ray maps for X_{Alm} and X_{Prp} display zoning inside the core. (f) Standardized X-ray map for X_{Sps}. The image appears fuzzy because Mn-contents are low. Note the areas with higher X_{Sps} in the core.

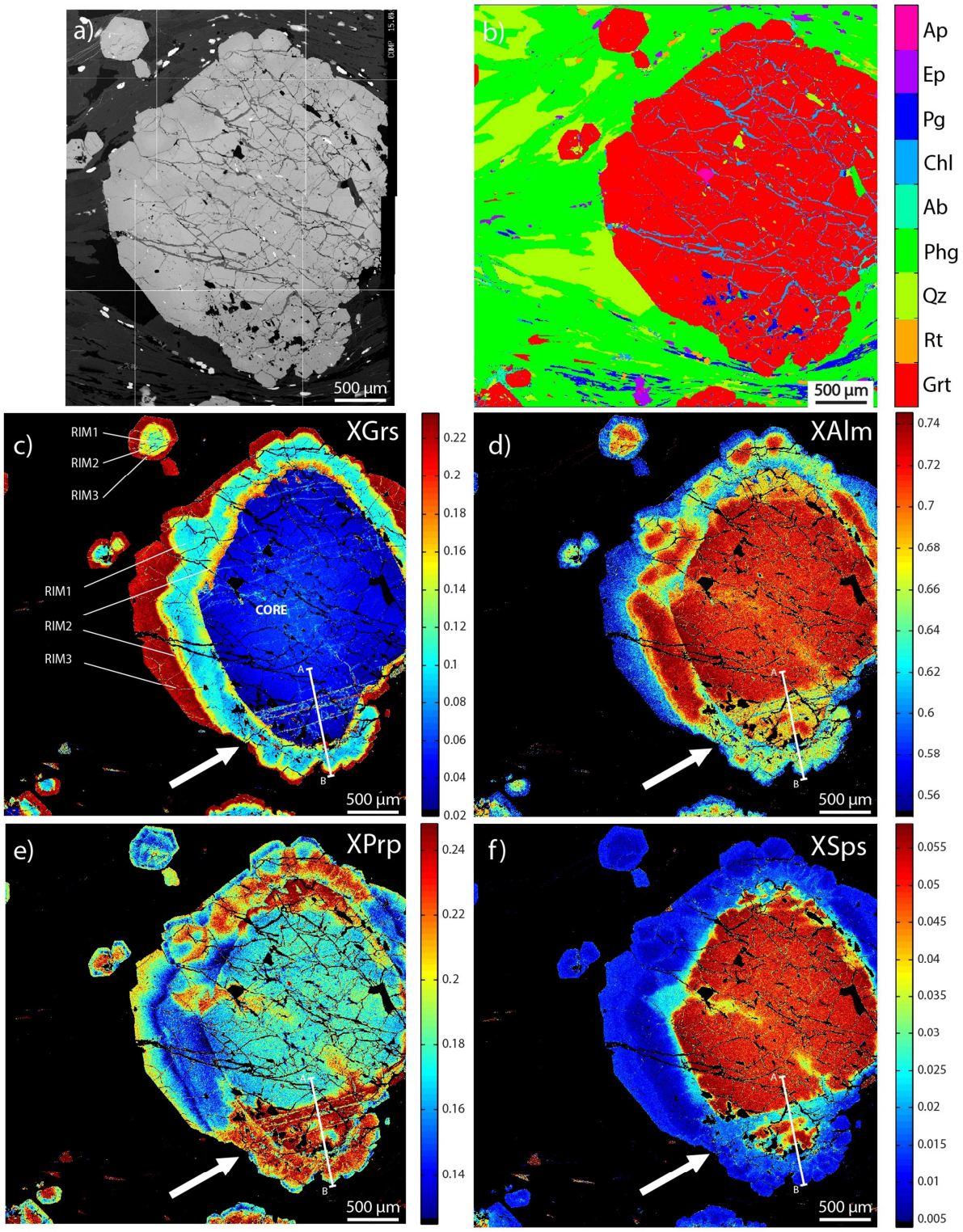
a)
500 µm
b)
Ap
Ep
Pg
Chl
Ab
Phg
Qz
Rt
Grt
500 µm
c)
XGrs
RIM1
RIM2
RIM3
RIM1
RIM2
RIM3
CORE
A
B
500 µm
0.22
0.2
0.18
0.16
0.14
0.12
0.1
0.08
0.06
0.04
0.02
d)
XAlm
A
B
500 µm
0.74
0.72
0.7
0.68
0.66
0.64
0.62
0.6
0.58
0.56
e)
XPrp
A
B
500 µm
0.24
0.22
0.2
0.18
0.16
0.14
f)
XSps
A
B
500 µm
0.055
0.05
0.045
0.04
0.035
0.03
0.025
0.02
0.015
0.01
0.005

Figure 7: Large garnet (ø ~3 mm) in sample FG1249. (a) BSE picture shows bright porphyroclastic core and darker rim. (b) Mineral phases (based on X-ray maps). Quartz is included inside the core and at the core-rim boundary, paragonite inclusions are abundant in correspondence of the major fractures sealed by higher grossular garnet. Late fractures that dissect all the garnet are filled by chlorite and albite. (c) X_{Grs} map. Major fractures are sealed by higher grossular garnet. Smaller garnet grains have no core but rims showing the same zoning. (d), (e) and (f). X_{Alm}, X_{Prp} and X_{Sps} maps, respectively, suggesting incipient re-equilibration in both core and Rim1 near major fractures (arrows) and along the core-Rim1 boundary (see text for discussion). Relics of the pristine core are preserved as islands inside re-equilibrated garnet Rim 2 and Rim3 (bottom part of figure). Note location of AB profile shown in Fig. 8.

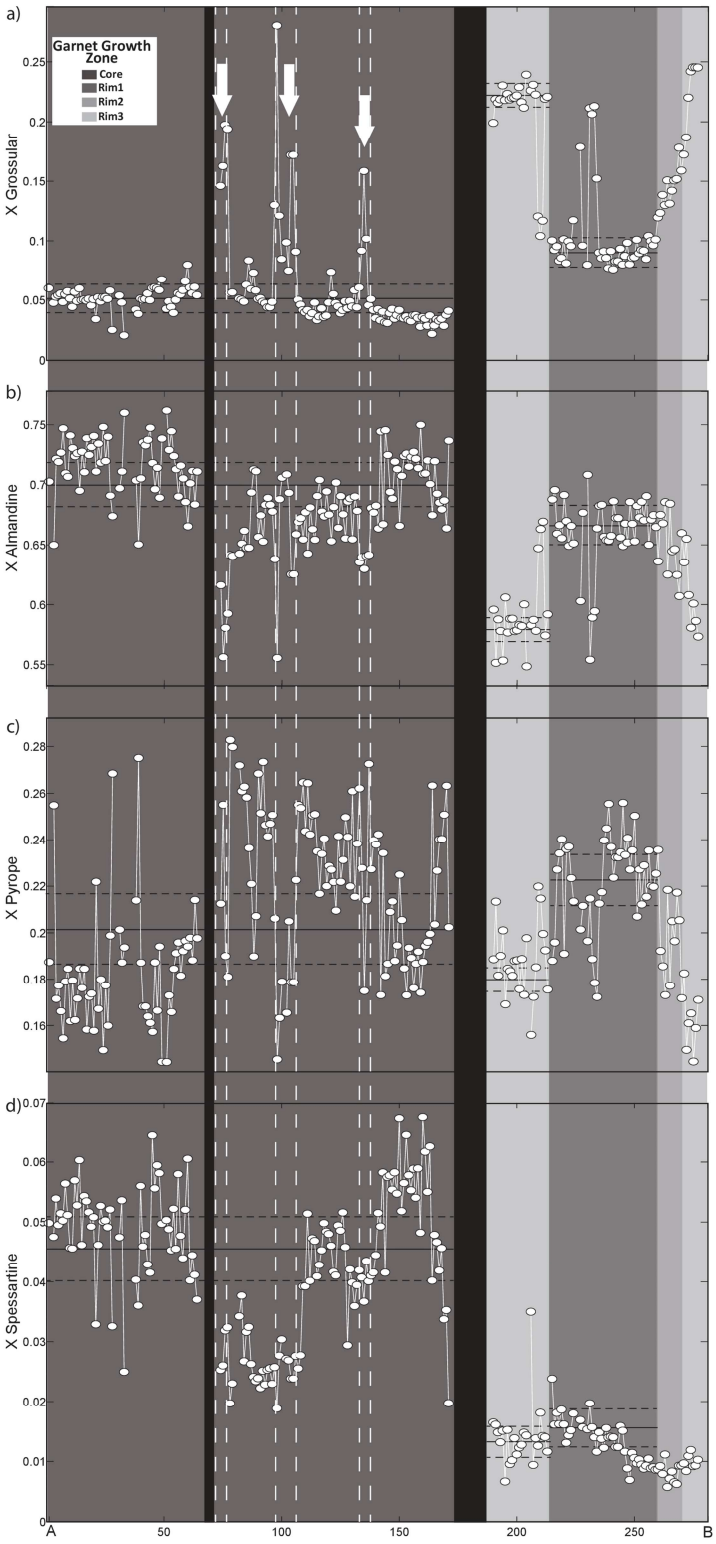
a)
Garnet Growth Zone
Core
Rim1
Rim2
Rim3
X Grossular
b)
X Almandine
c)
X Pyrope
d)
X Spessartine
A
B
50
100
150
200
250

Figure 8: Garnet end-member proportions along 300 µm profile (trace shown in Fig. 7) in sample FG1249. Note different mole fraction scales. Late chlorite fractures are highlighted by black bands. The fractures in the core, sealed by a garnet with different composition, are indicated by white arrows. Mean compositions are represented by black solid lines with the standard deviation (1σ) represented by the dashed black lines. (a) Grossular. (b) Almandine. (c) Pyrope. (d) Spessartine. The distinction of each garnet growth zone is based on its grossular content with the aim of helping the comparison.

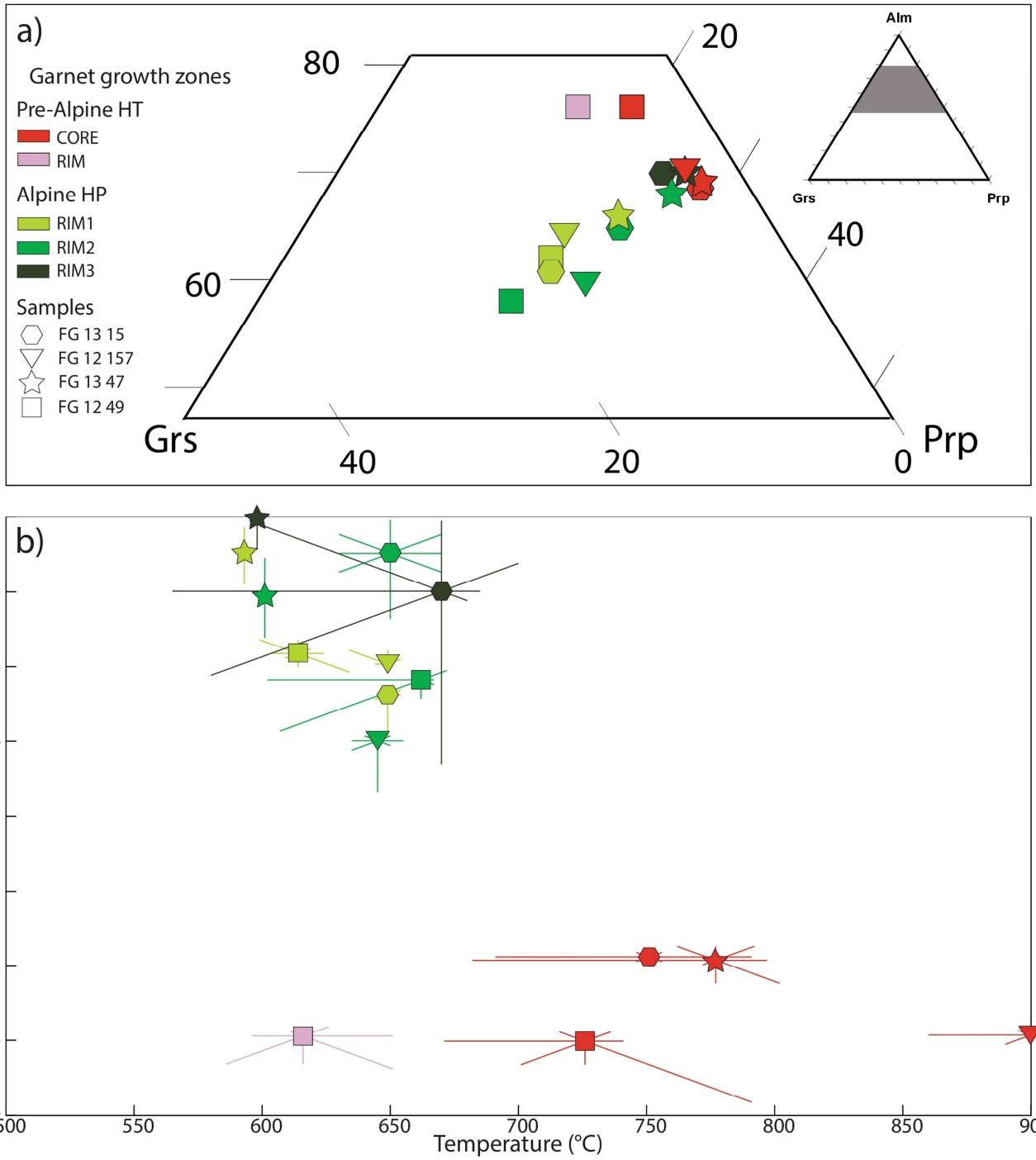

Figure 9: (a) End member diagram of the garnet growth zones from the four micaschists. (b) P-T diagram with a summary of the modelled conditions for each garnet growth zone. Note major difference in P-T conditions from the pre-Alpine to the Alpine generations. The effect of uncertainties in each set of isopleths is shown around the P-T

model of each growth zone (dataset from Lanari et al., 2017 and Giuntoli et al., in review) For sample FG1249 the pre-Alpine rim (pink) corresponds to Rim1, Rim 1 to Rim 2 and Rim 2 to Rim 3 in the text.

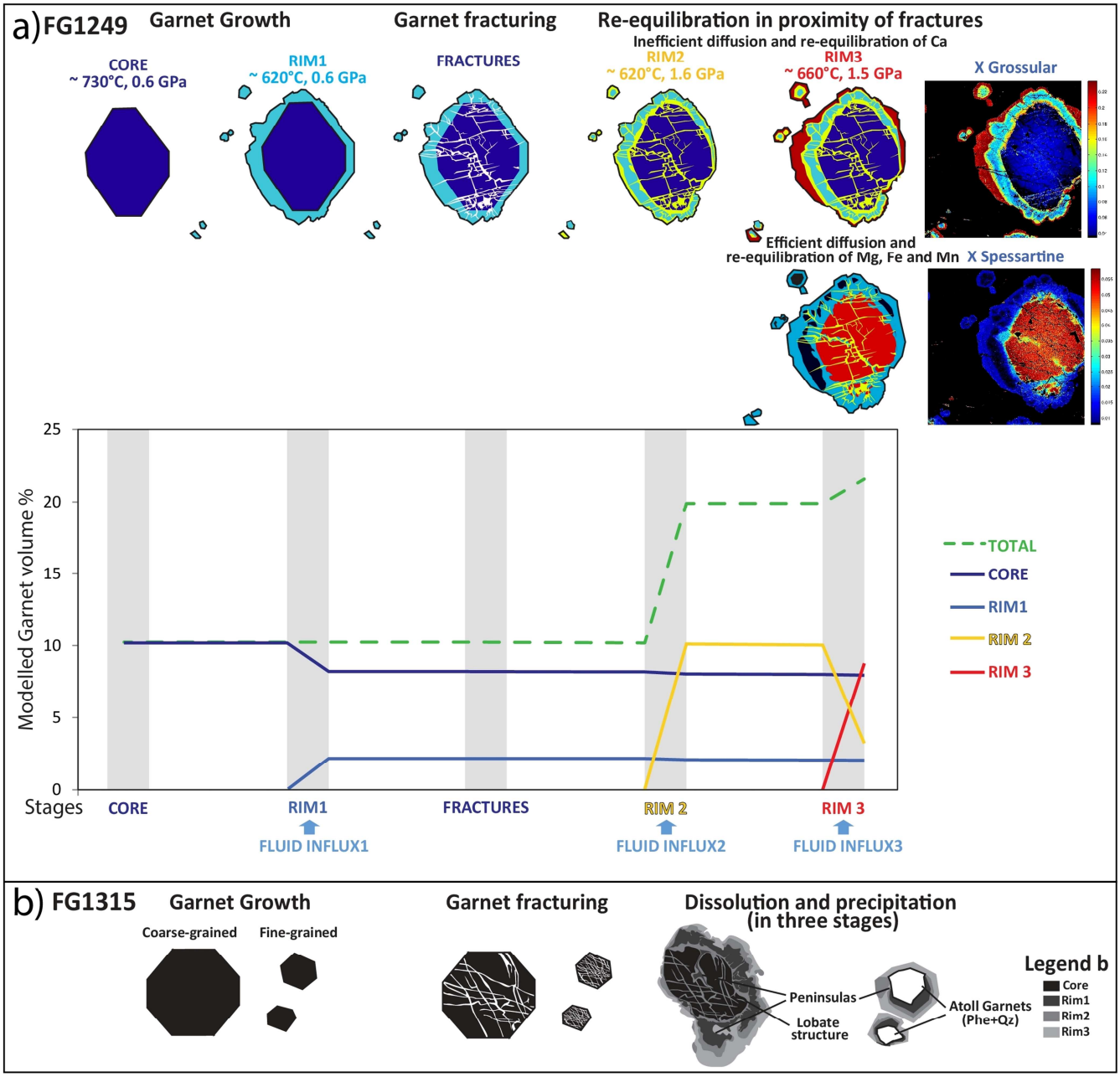

Figure 10: (a) Sketch illustrating the inferred chronology of sample FG1249, from textural observations and GrtMod thermodynamic modelling (see text for discussion). The preserved succession of stages in garnet evolution is shown along the abscissa, the modelled garnet volume along the ordinate; values include the sum total due to growth and resorption. Note the difference in P-T conditions for the core and Rim1 (both pre-Alpine), relative to Rim2 and 3 (both Alpine); the three fluid pulses are related to Rim1, 2 and 3 growths. After the growth of core and Rim1, a fracture network developed. In proximity of these fractures garnet core and Rim1 got effectively re-equilibrated due to diffusion of Mg, Fe and Mn, whereas Ca remained more immobile. (b) Sketch illustrating the sequence of processes inferred from garnet textures in samples FG1315. Fracture networks are visible in all the garnet core grain sizes. Subsequent stages of fluid influxes caused dissolution of the previous garnet generation/s and precipitation of new garnet, producing peninsulas, lobate structures and atoll structures in smaller garnet grains.

Sample	Minerals	Garnet growth zones	Sample locations
FG1315	Qz, Ph, Pg, Grt, Ep, Chl, Ab, Rt, Gr, Zrn	Pre-Alpine core + 3 Alpine rims. Note: atoll garnet	Rechantier, X= 408514, Y= 5051580
FG12157	Qz, Ph, Grt, Gln, Ep, Chl, Ab, Rt, Zrn, Ilm, Gr	Pre-Alpine core + 2 Alpine rims	Lillianes, X= 409683, Y= 5054033
FG1249	Qz, Ph, Pg, Grt, Ep, Chl, Ab, Rt, Gln, Zrn	Pre-Alpine core and Rim1 + 2 Alpine rims	Faye, X= 406637, Y= 5053931
FG1347	Qz, Ph, Pg, Cld, Grt, Ep, Chl, Rt, Zrn	Pre-Alpine core + 4 Alpine rims	Liévanere, X= 406318, Y= 5052474

Table1: Micaschists analysed (all from the Lys Valley). Mineral abbreviations from Whitney and Evans (2010). Coordinates refer to ED 1950 UTM Zone 32N.

Sample	FG1315				FG12157			FG1249				FG1347				
Garnet	**CORE**	**RIM 1**	**RIM 2**	**RIM 3**	**CORE**	**RIM 1**	**RIM 2**	**CORE**	**RIM 1**	**RIM 2**	**RIM 3**	**CORE**	**RIM 1**	**RIM 2**	**RIM 3**	**RIM 4**
Average composition (wt%)																
SiO2	37.70	37.96	37.81	37.44	38.17	38.43	38.74	36.91	36.62	37.80	37.98	37.75	37.88	38.18	37.75	37.33
TiO2	0.01	0.01	0.01	0.01	0.07	0.07	0.17	0.05	0.16	0.27	0.04	0.02	0.02	0.02	0.03	0.03
Al2O3	21.27	21.44	21.46	21.32	21.07	21.20	21.24	20.83	21.36	21.18	21.77	21.25	21.28	21.09	21.21	21.33
FeO	31.46	27.94	30.03	32.07	31.23	29.05	26.83	33.06	34.23	28.79	27.12	31.30	30.19	30.82	31.96	32.07
MnO	0.61	0.41	0.42	0.31	1.00	0.57	0.56	2.31	0.37	0.66	0.56	0.92	0.37	0.39	0.35	0.32
MgO	7.19	5.33	6.18	6.30	6.41	5.08	4.22	4.65	3.86	5.18	4.86	7.05	5.76	6.60	6.62	7.30
CaO	1.31	6.72	4.17	2.08	1.38	5.59	8.39	1.77	3.27	6.35	8.38	1.14	3.96	2.13	1.49	0.96
Cr2O3	0.00	0.00	0.00	0.00	0.04	0.04	0.04	0.03	0.04	0.03	0.03	0.00	0.00	0.00	0.00	0.00
Total	99.56	99.81	100.08	99.52	99.37	100.03	100.18	99.62	99.90	100.27	100.73	99.41	99.47	99.24	99.41	99.33
Formulae based on 12 oxygens																
Si	2.965	2.974	2.958	2.957	3.021	3.019	3.035	2.954	2.926	2.960	2.948	2.976	2.990	3.016	2.982	2.943
Ti	0.001	0.001	0.001	0.001	0.004	0.004	0.010	0.003	0.010	0.016	0.002	0.001	0.001	0.001	0.002	0.002
Al	1.972	1.980	1.979	1.985	1.965	1.963	1.961	1.965	2.011	1.955	1.991	1.974	1.979	1.964	1.975	1.981
Fe	2.069	1.831	1.965	2.119	2.067	1.908	1.758	2.213	2.287	1.885	1.760	2.064	1.992	2.035	2.111	2.114
Mn	0.041	0.027	0.028	0.021	0.067	0.038	0.037	0.157	0.025	0.044	0.037	0.061	0.025	0.026	0.023	0.022
Mg	0.843	0.623	0.720	0.741	0.756	0.595	0.493	0.555	0.459	0.605	0.563	0.828	0.677	0.777	0.780	0.858
Ca	0.110	0.564	0.350	0.176	0.117	0.470	0.704	0.152	0.280	0.533	0.697	0.096	0.335	0.180	0.126	0.081
∑ cations	8.001	8.000	8.000	8.000	7.997	7.998	7.997	7.998	7.998	7.998	7.998	8.000	7.999	7.999	7.999	8.000
Molecular proportions of garnet end members																
Alm	0.676	0.601	0.641	0.693	0.687	0.634	0.588	0.719	0.750	0.615	0.576	0.677	0.658	0.674	0.694	0.688
Prp	0.275	0.204	0.236	0.242	0.252	0.198	0.165	0.180	0.150	0.197	0.184	0.272	0.224	0.257	0.256	0.279
Grs	0.036	0.186	0.114	0.058	0.039	0.156	0.235	0.050	0.092	0.174	0.228	0.031	0.111	0.060	0.042	0.026
Sps	0.013	0.009	0.009	0.007	0.022	0.013	0.012	0.051	0.008	0.014	0.012	0.020	0.008	0.009	0.008	0.007

Table2: Representative analyses of garnet growth zones

S1 Additional sample information

S1.1 FG1315

Mode: quartz ~50%, micas (2/3 phengite, 1/3 paragonite) ~30%, garnet ~15%, remaining ~5% epidote, chlorite, albite, rutile, graphite and zircon.

This quartz-rich garnet micaschist was sampled at Rechantier, Lys Valley (Valle d'Aosta, Italy, Fig. S1; X= 408514, Y= 5051580, ED 1950 UTM Zone 32N).

Figure S1: Outcrop of sample FG1315. The shiny aspect on the XY plane is due to white mica. The stretching lineation is marked by the alignment of white mica and quartz.

S1.2 FG12157

Mode: quartz ~ 40%, phengite ~30%, garnet ~15%, ~10% glaucophane + epidote, accessory chlorite, albite, rutile, zircon, titanite, ilmenite, and graphite.

This glaucophane garnet micaschist was collected at Lillianes, Lys Valley (Valle d'Aosta, Italy, Fig. S2; X= 409683, Y= 5054033).

Figure S2: Outcrop photo of sample FG12157. Dark blue glaucophane, silvery phengite, is garnet, yellow epidote and white quartz.

S1.3 FG1249

Mode: quartz ~ 40%, micas (2/3 phengite, 1/3 paragonite) ~40%, garnet ~15%, accessory epidote, chlorite, albite, rutile, glaucophane, zircon, and opaques.

This garnet micaschist was sampled close to Faye, Lys Valley (Valle d'Aosta, Italy, Fig. S3; X= 406637, Y= 5053931).

Figure S3: Outcrop of sample FG1249. Note that centimetre-size garnet is wrapped by the intense foliation marked by white mica.

S1.4 FG1347

Mode: quartz ~35%, micas (mostly phengite with minor paragonite) ~25%, chloritoid ~15% garnet ~15%, remaining ~10% epidote, chlorite, rutile, opaques, and zircon.

This garnet chloritoid micaschist was sampled close to Liévanere above Pont-Saint Martin (Val d'Aosta, Italy, Fig. S4; X= 406318, Y= 5052474).

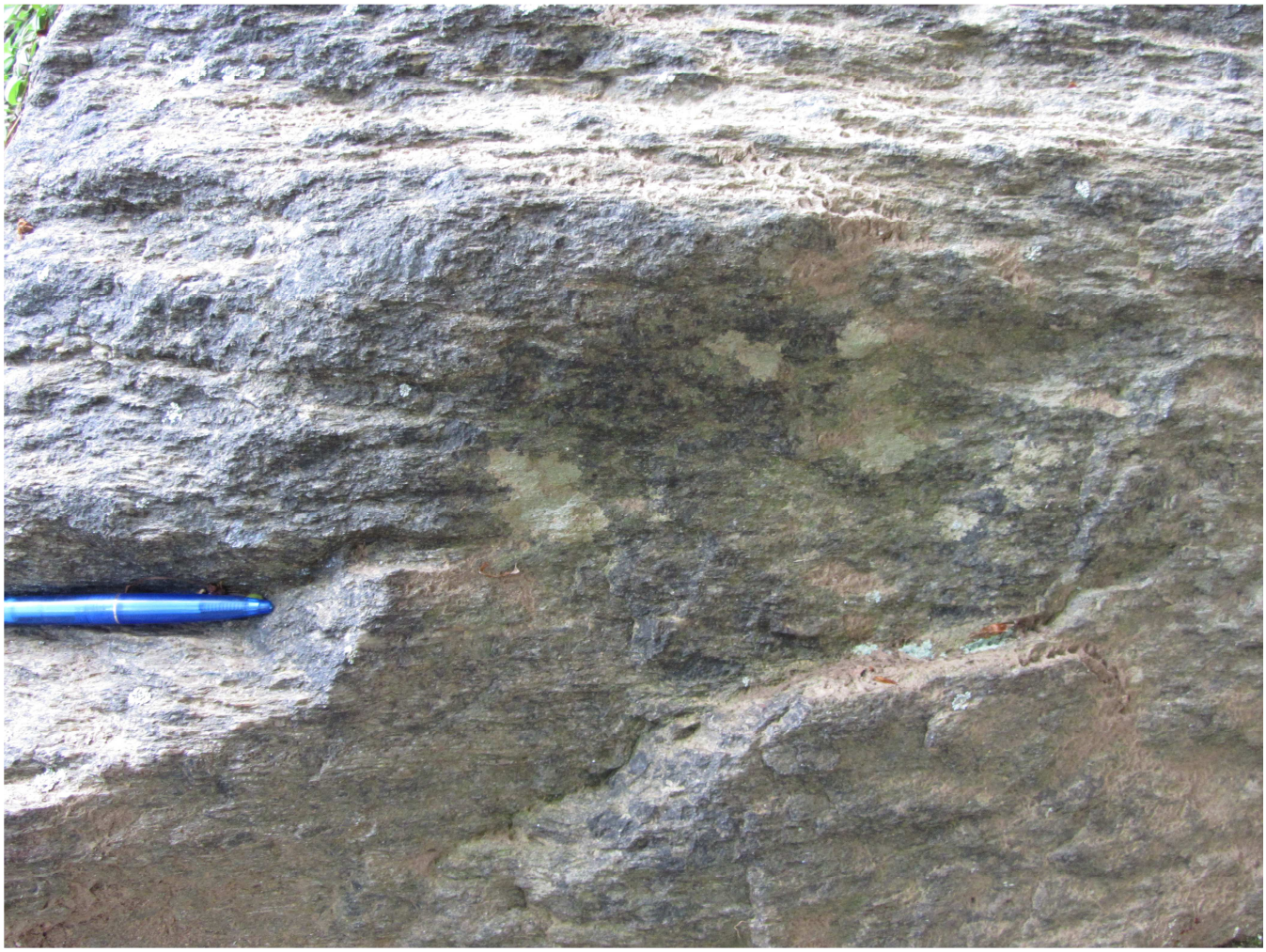

Figure S4: Outcrop photo of sample FG1347. The rusty red weathering colour is a typical feature of this lithotype. Chloritoid crystals up to 1 cm are grey in colour.

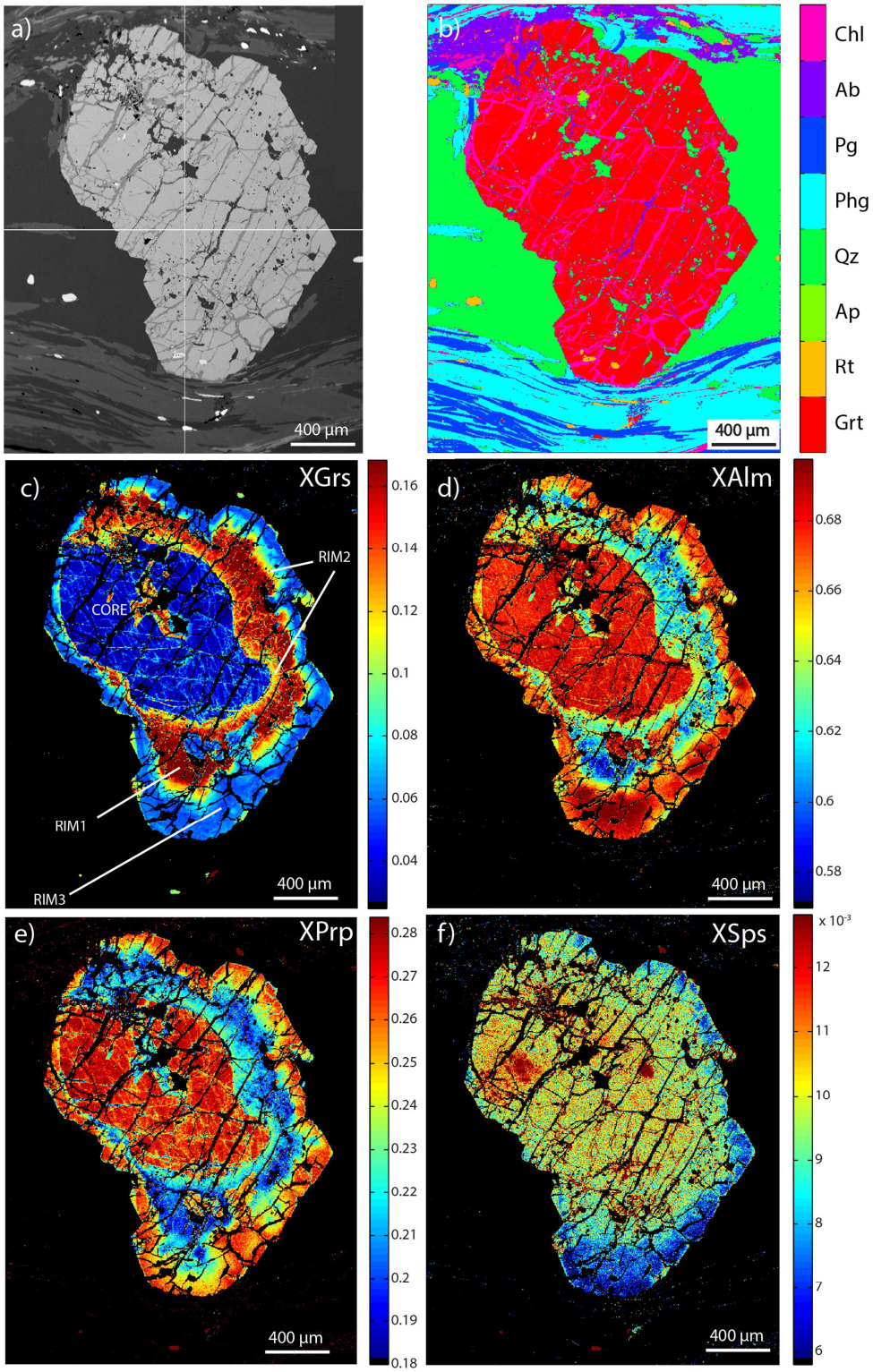
a)
400 µm
b)
400 µm
Chl
Ab
Pg
Phg
Qz
Ap
Rt
Grt
c)
XGrs
RIM2
CORE
RIM1
RIM3
400 µm
0.16
0.14
0.12
0.1
0.08
0.06
0.04
d)
XAlm
400 µm
0.68
0.66
0.64
0.62
0.6
0.58
e)
XPrp
400 µm
0.28
0.27
0.26
0.25
0.24
0.23
0.22
0.21
0.2
0.19
0.18
f)
XSps
400 µm
x 10-3
12
11
10
9
8
7
6

Figure S5: Large garnet (ø 1-2 mm) in sample FG1315. (a) BSE picture. (b) Mineral phases based on X-ray maps. Quartz inclusions are located inside Rim1 and between Rim1 and Rim3; rutile inclusions inside Rim3. Late fractures entirely dissect garnet and are filled by chlorite and albite. Garnet is located in a quartz rich band and is elongate perpendicular to the main foliation marked by phengite, paragonite and rutile. (c) Standardized X-ray map for X_{Grs} end-member. Note the lobate structure of the core, the pervasive fracture pattern sealed by garnet higher in X_{Grs} and the peninsula in which Rim1 and Rim2 grew. A fine network of veins is visible inside Rim1 and is sealed by Rim2. Rim3 produced two peninsulas inside Rim1 and Rim2. (d), (e) Standardized X ray maps for X_{Alm} and X_{Prp} show analogous features as in c. (f) Standardized X-ray map for X_{Sps}. Note two areas with higher X_{Sps}; the image is fuzzy because X_{Sps} values are low.

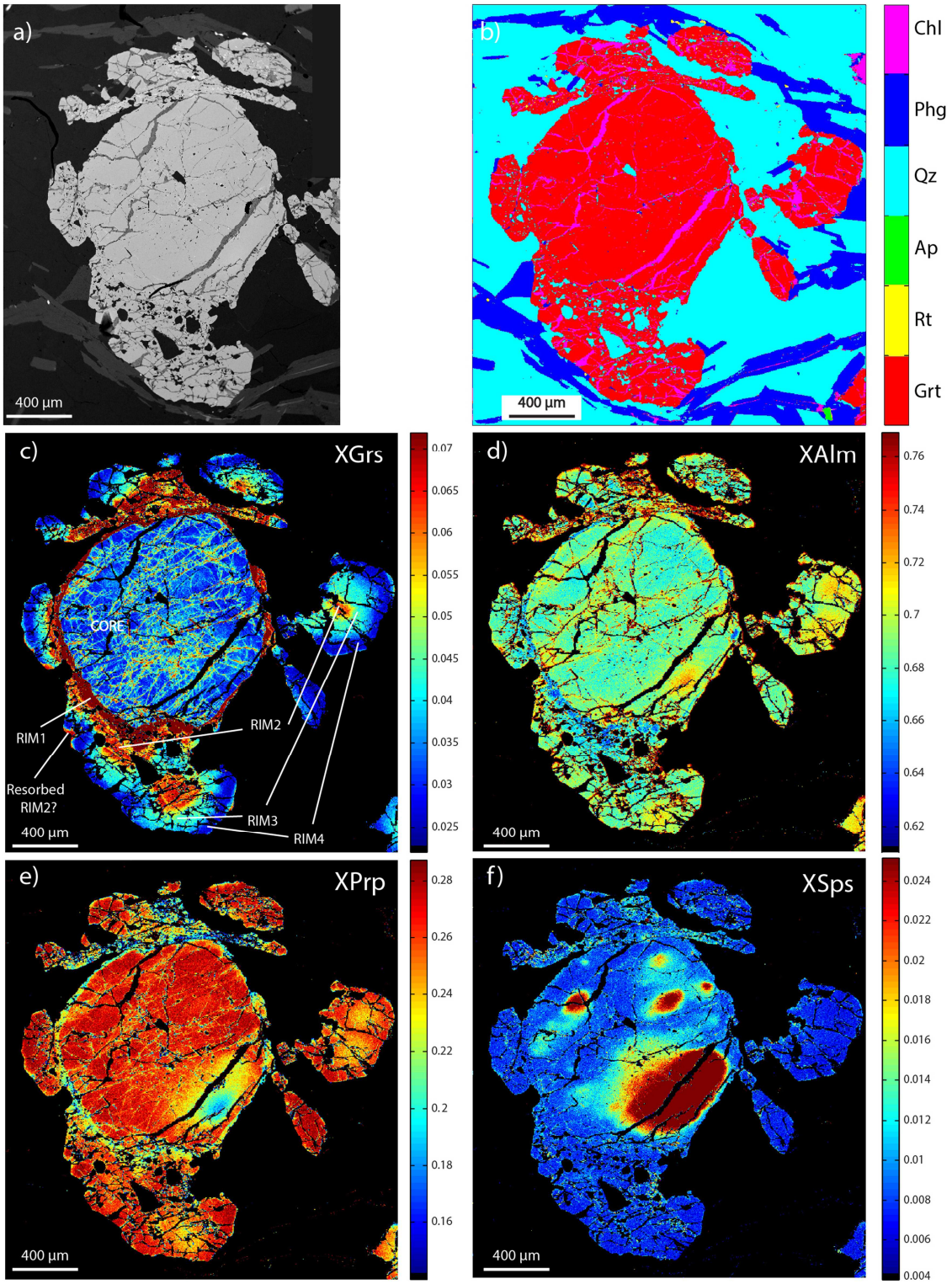
a)
400 µm
b)
400 µm
Chl
Phg
Qz
Ap
Rt
Grt
c)
XGrs
CORE
RIM1
RIM2
Resorbed
RIM2?
RIM3
RIM4
400 µm
0.07
0.065
0.06
0.055
0.05
0.045
0.04
0.035
0.03
0.025
d)
XAlm
400 µm
0.76
0.74
0.72
0.7
0.68
0.66
0.64
0.62
e)
XPrp
400 µm
0.28
0.26
0.24
0.22
0.2
0.18
0.16
f)
XSps
400 µm
0.024
0.022
0.02
0.018
0.016
0.014
0.012
0.01
0.008
0.006
0.004

Figure S6: Asymmetric zoning in mm-sized garnet from sample FG1347. (a) BSE picture with a bright porphyroclastic core and a darker rim rich in quartz inclusions. (b) Mineral phases based on X-ray maps. Garnet is located in a quartz-rich band wrapped by phengite that defines the main foliation. Quartz inclusions are present inside the rims. Late fractures dissect all of the garnet generations and are filled by chlorite. (c) Standardized X-ray map for the X_{Grs} end-member. Note the fractured core sealed by garnet with higher grossular content. Satellite garnet shows the same zoning except that the porphyroclastic core is missing. (d), (e) and (f) X_{Alm}, X_{Prp} and X_{Sps} maps showing zoning in the core, a feature not visible in the X_{Grs} map.

MAJOR ELEMENTS	SiO2	TiO2	Al2O3	Fe2O3	MnO	MgO	CaO	Na2O	K2O	P2O5	LOI	Cr2O3	NiO	Sum
	wt-%	wt-%	wt-%	wt-%	wt-%	wt-%	wt-%	wt-%	wt-%	wt-%	wt-%	wt-%	wt-%	wt-%
FG1315	64.09	0.95	17.12	7.78	0.08	2.34	0.72	1.05	3.13	0.10	2.06	0.01	0.01	99.43
FG12157	60.36	1.03	16.51	8.84	0.10	3.29	2.09	1.19	3.57	0.14	2.01	0.02	0.01	99.15
FG1249	58.82	1.03	18.87	9.58	0.23	2.76	1.60	0.88	3.94	0.13	1.58	0.02	0.01	99.44
FG1347	58.47	1.12	20.39	9.94	0.08	2.85	0.39	0.54	3.26	0.10	2.44	0.02	0.01	99.60

Table S1: Major element compositions of the studied samples